Data-Driven Optimizations of Manufacturing Processes

Anand Krishnan

A dissertation
submitted in partial fulfillment of the
requirements for the degree of

Doctor of Philosophy

University of Washington

2025

Reading Committee:
Krithika Manohar, Chair
Ashis G. Banerjee
Agnes Blom-Schieber

Program Authorized to Offer Degree:
Mechanical Engineering

University of Washington

Abstract

Data-Driven Optimizations of Manufacturing Processes

Anand Krishnan

Chair of the Supervisory Committee:
Krithika Manohar
Department of Mechanical Engineering

Despite the success of data-driven techniques in achieving superhuman performance across various domains, significant challenges remain in applying these methods to manufacturing processes. Unlike fields with large-scale datasets like ImageNet, manufacturing lacks comparable datasets to train machine learning models for tasks such as directly estimating ergonomic risk. Additional challenges, including sensor failures, limited data availability, and the time-intensive nature of data collection, constrain the performance and practical usability of machine learning models in this domain. These limitations highlight the need for tailored approaches that leverage domain-specific data and methodologies to address challenges unique to manufacturing.

Composite layup for small, complex parts is still done manually, presenting a compelling case for data-driven approaches due to the intricate motions and ergonomic risks involved. This work develops a data-driven ergonomic risk assessment system with a special focus on hand and finger activity to better identify and address ergonomic issues related to hand-intensive manufacturing processes. The system comprises a multi-modal sensor testbed designed to collect and synchronize data on operator upper body pose, hand pose, and applied forces. Ergonomic risk is assessed using the novel Biometric Assessment of Complete Hand (BACH) formulation to measure high-fidelity hand and finger risks, alongside industry-standard risk scores for upper body posture (RULA) and hand activity (HAL). Using the

collected dataset, machine learning models are developed to automate RULA and HAL scoring, achieving over 95% classification accuracy and generalizing well to unseen participants. The assessment system provides ergonomic interpretability of manufacturing processes and can be used to mitigate risks through workplace optimization and posture corrections.

Building on these human factors insights, this work investigates the transition from human-centered ergonomic assessment to large-scale manufacturing automation through data-driven methods. A hybrid correction framework is developed that combines Finite Element Model (FEM) simulations with experimental data, resulting in a computationally efficient approach for improved prediction accuracy. The approach achieves an average 91.9% reduction in RMSE compared to FEM predictions across eight actuator locations, with prediction uncertainties quantified to ensure model reliability. The corrected model is then applied to optimize actuator placement using QR decomposition of the displacement matrices, identifying optimal locations that achieve superior shape control performance compared to conventional placement strategies.

Looking ahead, the automated ergonomic risk assessment system and adaptive tooling techniques developed in this work establish a comprehensive framework for data-driven manufacturing optimization that addresses both human factors and system performance. The research demonstrates pathways for technology translation from laboratory demonstration to industrial deployment, representing a holistic approach to modern manufacturing challenges that prioritizes worker safety while enabling advanced automation capabilities.

DEDICATION

To Amma and Appa

ACKNOWLEDGMENTS

I express my sincere gratitude to my advisor, Professor Krithika Manohar, for her invaluable guidance, patience, and support throughout this research. Her expertise and mentorship have been instrumental in shaping both this work and my development as a researcher.

I thank my committee members—Professor Ashis G. Banerjee, Professor Adriana (Agnes) Blom-Schieber, and Professor Sam Burden—for their insightful feedback and constructive suggestions that significantly improved this dissertation.

I am particularly grateful to Professors Ashis Banerjee and Santosh Devasia, whose advice continues to guide my approach to research problems and evaluation of results. I also acknowledge the exceptional mentorship from Boeing collaborators. First and foremost, I would like to thank Dr. Agnes Blom-Schieber, who taught me to pursue meaningful, impactful research through her hands-on problem-solving approach. I also thank Monica Tatar, Jonathan M. Jeyachandran, Jonathan Y. Ahn, Richard Gardner, Samuel F. Pedigo, and Shuonan Dong for their valuable contributions. Finally, I would like to thank my research collaborators, Xingjian Yang, Ricardo Herrera, Henry Chang, Mohamed Safwat, Benjamin Wong, Kaleb Yohannes, and Utsav Seth.

To my parents, Srinivasa Radha Krishnan and Veena Ghaty Seetharam, thank you for your endless support and for giving me the privilege of pursuing my academic dreams. I have also been fortunate to have my family in the same city for the entire duration of my graduate studies. To my sister Nikhila Krishnan, brother-in-law Sushanth Kumar, and dear nephew Himay Nishanth (who was born when I started my PhD), your support means the world to me and this truly would not have been possible without you. I am especially grateful to Niharika Karnik. You have worn many hats, including best friend, lab mate, hiking buddy,

rant partner, and the list goes on and on. Thank you for always being in my corner when the whirlwinds of graduate studies threatened to blow me away.

Coming from India, the friends you make in a new country quickly become your family. I am also deeply grateful to all my friends. During my PhD, Aditya Ashok, Nithya Chandran, Clarissa Bargellini, Charlie Legge, Rahul Mayuranath, Poojita Raj, Aparijit Venkatesh, Srinithya Nagarajan, and Thomas Chu ensured I laughed and enjoyed my weekends. During my Masters, I cannot forget the wonderful Friday nights with Anand Krishnan Srikanth, Shreyas Shetty, Mark Ghali, and Duc (Tony) Nguyen which kept me going through the pandemic. Last but not least, I appreciate Sumedha Biswas, Vishwajeet Nadgouda, Sachin Bhardwaj, and Amatullah Yousuf for staying friends with me even across oceans.

In the lab, I am thankful to Jan Williams, Andrei Klishin, Nick Zolman, Dima Tretiak, Sajeda Mokbel, Sam Ahnert, Kartik Krishna, Chinmay Ratnaparkhe, and Yash Bhangale for always making me feel like there was a community at work to bounce ideas off of, discuss overrated and underrated techniques, and generally do graduate student stuff with. Special thanks to the participants who volunteered for the data collection studies. Their contributions made this work possible.

This work was supported by the Joint Center for Aerospace Technology Innovation (JCATI) and the National Science Foundation AI Institute in Dynamic Systems (grant number 2112085).

TABLE OF CONTENTS

LIST OF FIGURES

LIST OF TABLES

Chapter 1

INTRODUCTION

1.1 Evolution of Manufacturing Processes and Materials

The evolution of manufacturing processes has been a cornerstone of human progress, driving innovation and reshaping industries. From the mechanization of the Industrial Revolution to the advent of advanced materials in the 20th century and the digital transformation of the 21st century, manufacturing has continually adapted to meet the demands of a changing world. This evolution is particularly evident in aerospace manufacturing, where the shift from metals to composite materials has created opportunities for innovation while introducing significant challenges. In the modern context, data-driven methodologies have emerged as a powerful tool, not only enhancing these processes but also addressing inefficiencies that have persisted across generations of manufacturing advancements.

The Industrial Revolution catalyzed the first major transformation in manufacturing, introducing mechanization through technologies such as the steam engine and mechanized textile production [53]. Factories became hubs of innovation, enabling mass production through interchangeable parts and assembly lines [34]. This period established metals—iron and steel in particular—as the dominant materials for manufacturing, prized for their strength, durability, and availability. The reliance on metals allowed industries to achieve unprecedented scalability, but it also limited the range of applications where lightweight or corrosion resistance was critical. These advancements not only accelerated industrial output but also created the foundation for modern manufacturing practices, fostering urbanization and reshaping global economies.

The 20th century brought transformative advancements in manufacturing processes, including automation, precision machining, and the development of new materials such as

composites. Composites—engineered by combining materials to create superior mechanical properties—gained prominence in aerospace manufacturing for their ability to reduce weight while maintaining strength and resistance to fatigue [66]. Despite these advantages, their adoption presented several challenges, such as higher production costs, complex processing requirements, and limited recycling options. These difficulties underscored the need for innovative approaches to optimize composite manufacturing and ensure scalability for aerospace applications.

In the 21st century, advancements in digital technologies and data-driven methodologies have begun to address the inherent challenges of manufacturing. Industry 4.0 principles, such as the integration of artificial intelligence (AI), machine learning, and the Internet of Things (IoT), have enabled aerospace manufacturers to improve precision, reduce waste, and enhance product quality [60]. Additive manufacturing has also played a pivotal role in composite production, enabling complex geometries and reducing material waste. These advancements have not only revolutionized production processes but also shifted the focus toward adaptive, real-time monitoring of manufacturing systems. Incorporating data-driven analysis allows for the use of large-scale data from sensors, simulations, and process monitoring to optimize workflows and predict material behavior.

This sets the stage for a deeper examination of how data-driven augmentations can address these challenges posed by modern composite manufacturing. Additionally, advancements in human-centric technologies, such as ergonomic analysis, are bridging gaps in tasks that remain human-intensive such as composite hand layup. For example, data-driven insights can help assess and reduce ergonomic risks, allowing manufacturers to learn and refine human motion for automation in composite layup processes. These approaches not only enhance efficiency and reduce injuries and associated costs but also contribute to the development of sustainable and resilient production systems. The subsequent sections will delve into data-driven analysis and machine learning techniques, highlighting their transformative potential for optimizing composite manufacturing workflows and advancing the field.

1.2 Data-Driven Analysis using Machine Learning

The advent of data-driven discovery marks a significant shift in how science and engineering tackle complex problems. This shift, referred to as the "fourth paradigm" of scientific discovery, complements traditional empirical, theoretical, and computational approaches [8]. In this paradigm, data serves as the primary resource for understanding, modeling, and predicting phenomena, often revealing insights that would otherwise remain obscured. This approach has been fueled by advancements in computational techniques and a deluge of data from sensors, simulations, and experiments, enabling researchers to explore new frontiers in engineering, physics, and manufacturing processes.

The rise of machine learning (ML) as a cornerstone of data-driven discovery is closely tied to the increasing availability of data and advancements in computational resources. The growth of large-scale digital datasets in the 2000s, alongside advancements in high-performance computing (HPC) and the emergence of graphics processing units (GPUs), enabled training of increasingly complex ML models [55]. The proliferation of cloud computing further democratized access to computational power, allowing industries and researchers alike to harness the potential of machine learning. These developments made it possible to extract meaningful patterns from vast datasets, enabling ML techniques to gain prominence across scientific and industrial domains.

The trajectory of ML has been marked by milestones that underscore its impact on diverse fields. In 1997, IBM's Deep Blue defeated chess grandmaster Garry Kasparov, showcasing the potential of algorithmic computation [11]. By the mid-2010s, deep learning took center stage as AlphaGo achieved superhuman performance in the complex game of Go by combining reinforcement learning with neural networks [100]. Advances in convolutional neural networks (CNNs) revolutionized image recognition, demonstrated by breakthroughs in the ImageNet competition, where classifiers achieved human-level accuracy and beyond [51, 40]. These advances extended beyond games and image processing, with recurrent neural networks (RNNs) and transformers paving the way for natural language processing [111]. Today,

large language models (LLMs) like GPT and BERT exhibit exceptional performance in tasks ranging from translation to summarization, representing a leap forward in understanding and generating human-like text [6].

Improvements in sensing technology has also drastically enhanced the quality and quantity of data available. High-resolution sensors, multimodal sensing systems, and real-time data acquisition platforms provide unprecedented granularity in observing physical processes. In manufacturing, this has enabled detailed study of both automated workflows and human interactions, generating actionable insights for process optimization. For instance, advancements in machine vision and edge computing allow ML systems to monitor production lines and detect defects in real-time, significantly improving quality control.

Despite these advancements, directly applying ML techniques to manufacturing remains a significant challenge. Unlike domains like image recognition or language processing, manufacturing lacks large, publicly available datasets or standardized benchmarks for comparing model performance. Sensor failures, noisy data, and domain-specific complexities add further challenges. Moreover, safety-critical applications, such as aerospace manufacturing, require robust uncertainty quantification to ensure reliability and compliance with stringent standards. These hurdles highlight the need for customized ML methodologies that integrate domain knowledge with data-driven insights.

In the following sections, we will explore how data-driven manufacturing is addressing these challenges. By using custom datasets, tailored modeling techniques, and approaches that integrate physics-based knowledge with machine learning, researchers and industries are working to improve the efficiency and reliability of manufacturing systems. This transition represents an important step in applying machine learning to manufacturing, enabling more efficient processes and practical improvements.

1.3 Data-Driven Manufacturing

The integration of data-driven techniques in manufacturing has led to significant advancements in efficiency, quality control, and process optimization. Modern manufacturing systems leverage vast amounts of data collected from sensors, machines, and production lines to gain actionable insights. As outlined in [85], big data analytics has become central to intelligent manufacturing systems, providing tools for real-time decision-making and predictive maintenance. The systematic mapping study highlights how data integration across systems enables manufacturers to identify inefficiencies, streamline operations, and adapt to dynamic production environments. Similarly, data-driven smart manufacturing frameworks use advanced analytics to interconnect physical and digital spaces, creating intelligent systems that respond to real-time conditions while ensuring resource efficiency [106].

The role of data in manufacturing extends beyond operational improvements. Large-scale data aggregation enables comprehensive supply chain management, allowing manufacturers to predict market demands and adjust production accordingly [85]. Furthermore, integrating artificial intelligence (AI) techniques into these frameworks enables predictive capabilities and adaptive process control [106]. The convergence of IoT devices, cloud platforms, and big data analytics in manufacturing systems exemplifies a shift toward more responsive and resilient production environments. These advances provide manufacturers with the tools to meet increasing demands for customization and sustainability.

Machine learning (ML) techniques have further enhanced the capabilities of data-driven manufacturing systems. ML offers significant advantages in pattern recognition, anomaly detection, and process optimization. For instance, supervised learning algorithms are employed to detect defects in real-time, reducing production waste and ensuring quality standards. Unsupervised learning methods, on the other hand, help identify previously unnoticed patterns in production data, enabling predictive maintenance and minimizing machine downtime [118]. Similarly, [25] illustrates the diverse applications of ML, from energy consumption prediction to production scheduling. Despite these advancements, challenges such as limited

data availability in specific domains and the need for robust models capable of handling noisy data remain key obstacles.

In the context of composite materials, machine learning has emerged as a valuable tool for addressing the complexity of their manufacturing processes. Composite materials often involve intricate interactions between components, making traditional process optimization methods challenging. ML techniques have been employed to predict material properties, optimize curing processes, and reduce defects in composite layups. Studies have demonstrated the ability of neural networks and regression models to predict strength and stiffness based on manufacturing parameters, enabling more precise control of production.

ML is increasingly recognized for its transformative role in aerospace engineering, particularly in addressing the complexities inherent in aerodynamic modeling, system control, and structural analysis. As discussed in "Data-Driven Aerospace Engineering: Reframing the Industry with Machine Learning" [9], ML techniques like deep learning, regression analysis, and reinforcement learning are employed to create computationally efficient models for high-dimensional systems, such as fluid dynamics and coupled structural interactions. These models serve as viable alternatives or supplements to traditional, computationally intensive approaches, allowing for real-time optimization and decision-making, which are crucial in the design and operational phases of aerospace systems. The use of sparsity-promoting methods, such as sparse identification of nonlinear dynamics (SINDy) [10], helps derive governing equations directly from data, enhancing model interpretability and reducing the need for high-fidelity simulations.

Furthermore, the integration of data-driven approaches with classical physics-based modeling creates hybrid systems that leverage the strengths of both paradigms. Such hybrid models retain the physical accuracy of traditional techniques while gaining the adaptability and efficiency provided by machine learning, leading to more robust and adaptable aerospace solutions. One such avenue is optimal sensor and actuator placement using balanced model reduction. The importance of leveraging underlying patterns in physical systems for effective sensor placement is emphasized in [70]. By exploiting these known spatial or temporal

patterns, sparse sensor configurations can be designed to optimally reconstruct the system's state using fewer measurements. This data-driven sensor placement strategy not only reduces the computational and logistical burden associated with large sensor networks but also significantly improves the efficiency of monitoring and control processes.

In addition, balanced truncation techniques to identify the most critical states of a system facilitate the strategic placement of sensors and actuators to enhance system controllability and observability [71]. This approach effectively reduces system complexity while ensuring that the key dynamics are accurately captured and controlled. Together, these methods contribute to the development of efficient, cost-effective, and highly reliable sensing strategies in aerospace applications, ultimately enhancing overall system performance.

1.4 Motivation and Challenges

1.4.1 Ergonomics as a measure of manufacturing productivity and sustainability

Hand-intensive manufacturing processes are essential in specialized industries such as textile draping, precision leatherwork, fine carpentry, and decorative artwork. This is particularly true in aerospace composites manufacturing, where increasing demand has surpassed the capacity of automated solutions. Although machines such as Automated Fiber Placement (AFP) machines are capable of laying large composite parts such as wing panels, they are unsuitable for creating smaller and more complex geometric components that involve intricate features like narrow channels or transitions from convex to concave surfaces, such as hat stringers [52]. These intricate parts, for now, can only be produced by skilled operators during hand layup, where workers use visual and tactile feedback to carefully position the material, apply force, and make continuous adjustments to ensure proper adhesion. This process is repeated until the required gauge thickness is achieved. Unlike automated machines, humans bring adaptability, making on-the-fly adjustments to force and motion that are crucial for such detailed tasks.

Ergonomics plays a crucial role in bridging the gap between sustainability and productiv-

ity in manufacturing environments. By designing workspaces and processes that prioritize the physical well-being of workers, ergonomics helps reduce the risk of injury, minimize fatigue, and enhance overall worker satisfaction—all of which contribute to sustainable operations. A well-considered ergonomic approach not only improves individual health outcomes but also leads to fewer disruptions, less downtime, and greater workforce efficiency. This dual focus on worker health and operational performance makes ergonomics an essential factor in creating resilient and productive manufacturing systems that prioritize both human welfare and long-term sustainability goals.

Hand-intensive tasks pose significant ergonomic risks to workers, particularly due to the repetitive actions and forceful exertions required. The physical demands of hand layup, combined with spatial constraints and the need for precise adjustments, can lead to musculoskeletal disorders and long-term health issues for operators. Spatial constraints and task complexity further exacerbate these risks, as characterized by the Index of Difficulty (ID), which along with movement speed and accuracy can be used to model the challenges faced by operators [24]. In addition, age and physical capacity can impact task performance, especially for older operators who may experience reduced movement adaptability [62]. Stochastic models can further capture the complexity of these tasks by considering both environmental factors (e.g., spatial constraints, tool dimensions, etc.) and operator-specific traits (e.g., strength, reach, etc.) to assess how such variables influence task speed and difficulty [63]. There is a clear need for a comprehensive data-driven approach that not only captures the unique skills of human operators but also effectively assesses and predicts ergonomic risks to enhance safety and efficiency in the manufacturing workplace.

1.4.2 Adaptive Tooling in Digital Twin Augmentation

Flexible structures in manufacturing applications often exhibit shape variations when assembled or loaded, presenting challenges that result in lengthy measurement, adjustment, and inspection processes during production. These deviations from nominal configurations can significantly impact manufacturing efficiency and product quality.

Composite flexible structures can be modeled using finite element methods (FEM), which provide information about structural deflection at specified locations when applying specific forces with given boundary conditions. By combining the physics-based understanding from FEM models with experimental measurement data from the actual structures, the objective is to develop a hybrid model that captures the discrepancy between predicted and observed behavior. This approach results in a customized, accurate, and computationally efficient modeling framework.

The hybrid model serves as the foundation for actuator optimization strategies. QR decomposition of the displacement matrix derived from FEM analysis identifies optimal locations for actuator placement, corresponding to regions of maximum controllability associated with the principal modes of structural deformation. This systematic approach enables determination of the optimal number and placement of actuators required to achieve specified shape control objectives.

Challenges in this domain include varying structural stiffness due to manufacturing variations, fasteners, and reinforcement elements, as well as geometric differences across individual components that require customized control strategies. To address these challenges, the research aims to automate actuator quantity and placement decisions, enabling automated shape control through a general framework that augments computationally efficient nominal finite element models with experimental measurement data.

1.5 Organization

The remainder of this dissertation is structured as follows. Chapter 2 provides a comprehensive literature review covering composite manufacturing processes, ergonomic assessment methodologies in manufacturing environments, adaptive learning systems, digital twin technologies, and optimal actuator placement strategies. Chapter 3 presents the development of a multimodal sensing testbed for collecting operator data during hand-intensive manufacturing tasks, establishes industry-standard ergonomic risk assessment frameworks including RULA and HAL scoring, and introduces the novel Biometric Assessment of Complete

Hand (BACH) methodology. Chapter 4 describes the development and validation of machine learning models that automate RULA and HAL scoring with robust generalization to unseen participants, completing the ergonomic risk assessment framework. Chapter 5 addresses the transition from human factors to large-scale manufacturing automation, demonstrating how ergonomic assessment drives automation needs while establishing hybrid physics-data approaches for flexible structure control that achieve significant improvements over traditional finite element methods. Finally, Chapter 6 presents the overall contributions to data-driven manufacturing optimization and outlines future research directions, including technology translation pathways for ergonomic monitoring systems and extended validation frameworks for adaptive shape control technologies.

Chapter 2

LITERATURE REVIEW

2.1 Advances in Composite Manufacturing using Machine Learning

Composite manufacturing involves the production of materials made from two or more distinct constituents, typically a reinforcement and a matrix, resulting in superior mechanical, thermal, and chemical properties compared to their individual components. These materials are widely used in industries such as aerospace, automotive, and energy due to their lightweight nature and high strength-to-weight ratios. Recent advancements have increasingly focused on integrating data-driven approaches and machine learning to optimize processes, predict material behavior, and enhance manufacturing efficiency.

The adoption of machine learning in composite manufacturing was driven by limitations inherent in conventional analytical and numerical approaches. Traditional methods for predicting composite properties and optimizing manufacturing processes often required extensive experimental trials or computationally expensive simulations. Machine learning techniques offered the ability to capture complex, nonlinear relationships between processing parameters and material properties that were difficult to model using conventional approaches. Furthermore, ML methods enabled rapid property prediction and process optimization using data from previous experiments or simulations, reducing the need for costly physical testing and iterative design cycles.

Early applications of neural networks established the foundation for data-driven composite manufacturing. [110] demonstrated the use of back-propagation neural networks for delamination prediction in composite beams, establishing frameworks for structural health monitoring. Similarly, [64] integrated resin transfer molding (RTM) virtual manufacturing simulation with neural network-genetic algorithm optimization, creating process models for

predicting resin flow patterns and processing efficiency. These foundational approaches were expanded by [45], who applied neural networks for predicting tribological properties of polymer composites, and [5], who used artificial neural networks to predict kinetic parameters in carbon fiber reinforced composites for process parameter optimization.

The integration of machine learning with advanced manufacturing processes has led to comprehensive automation frameworks. [7] developed automation systems for automated fiber placement (AFP) processes that integrate process data from planning, computer numerical control (CNC), and online process monitoring for automated generation of manufacturing knowledge. These approaches have been complemented by advances in sensor technology, where [74] demonstrated the use of nanomaterial-based piezoresistive sensors to monitor and optimize manufacturing processes.

Deep learning architectures have enabled significant advances in composite property prediction and design optimization. [36] applied convolutional neural networks to predict composite material properties and design hierarchical composites through ML-driven optimization. This work was extended by [35], who developed ML algorithms for de novo composite design, enabling discovery of high-performance materials with optimal mechanical properties. A comprehensive framework for these approaches was provided by [17], who reviewed linear regression, neural networks, CNNs, and Gaussian processes for property prediction and design optimization.

Generative modeling approaches have emerged as powerful tools for inverse materials design. [18] developed deep neural networks for inverse design of materials using backpropagation and active learning strategies. Building on this foundation, [119] enabled mechanical property prediction directly from microstructural images by developing CNNs that predict stress-strain curves of composite microstructures. Advanced deep learning models have been demonstrated by [120], who used conditional generative adversarial networks to predict stress and strain fields directly from material microstructure geometry.

The progression from basic neural networks to physics-guided neural operators demonstrates substantial development in the field. Deep learning architectures have enabled com-

posite property prediction from microstructural images, while digital twin technologies provide real-time process monitoring and predictive maintenance capabilities. Computer vision systems achieve pixel-level defect detection in manufacturing environments, and physics-guided neural networks combine domain knowledge with data-driven approaches for improved accuracy with limited training data.

Despite these advances in automated composite manufacturing systems, a significant portion of composite production, particularly for complex geometries and specialized applications, continues to rely heavily on human operators. As noted by [52], although machines such as Automated Fiber Placement (AFP) machines are capable of laying large composite parts such as wing panels, they are unsuitable for creating smaller and more complex geometric components that involve intricate features like narrow channels or transitions from convex to concave surfaces, such as hat stringers. Hand-intensive processes such as composite layup for intricate aerospace components remain predominantly manual due to the adaptability and dexterous capabilities that human workers provide. While machine learning has transformed the technological aspects of composite manufacturing, ensuring the safety, health, and ergonomic well-being of human operators represents an equally critical dimension of sustainable and productive manufacturing systems. This human-centric perspective becomes essential when considering that manufacturing sustainability encompasses not only technological efficiency but also workforce health and safety, leading to the need for comprehensive ergonomic risk assessment and mitigation strategies in composite manufacturing environments.

2.2 Ergonomic Assessment in Manufacturing

Ergonomics, defined by the International Ergonomics Association as the scientific discipline concerned with understanding interactions among humans and other elements of a system, represents a critical component of modern manufacturing design and optimization [15]. The field encompasses the application of theory, principles, data, and methods to design in order to optimize human well-being and overall system performance [94]. In industrial contexts,

ergonomic considerations directly impact worker health, productivity, safety, and manufacturing sustainability. The economic significance of ergonomic factors in manufacturing is substantial, with musculoskeletal disorders (MSDs) representing one of the leading causes of workplace injury and associated costs [109]. According to occupational safety and health administration data, work-related MSDs account for approximately one-third of all workplace injuries and illnesses, resulting in significant direct and indirect costs including medical expenses, workers' compensation claims, reduced productivity, and increased absenteeism [83].

The historical development of ergonomic awareness in industrial settings can be traced through several distinct phases of scientific and practical advancement. Early industrial engineering efforts, pioneered by Frederick Winslow Taylor and Frank and Lillian Gilbreth in the early 20th century, established foundational principles of work study and motion analysis [107, 32]. These early approaches, while primarily focused on efficiency optimization, laid groundwork for understanding human factors in manufacturing processes. The Hawthorne studies conducted between 1924 and 1932 demonstrated the importance of considering human psychological and social factors in workplace design [73]. World War II catalyzed significant advancement in human factors engineering, as complex military systems required careful consideration of human-machine interfaces and operator capabilities [16]. Post-war industrial development incorporated these lessons, leading to systematic approaches for evaluating and improving workplace ergonomics. The establishment of regulatory frameworks, including the Occupational Safety and Health Act of 1970 in the United States and subsequent international standards development through the International Organization for Standardization, formalized requirements for ergonomic consideration in workplace design.

Contemporary ergonomic assessment methodologies have evolved to provide systematic approaches for evaluating workplace risks and developing intervention strategies. The Rapid Upper Limb Assessment (RULA) [75] and Hand Activity Level (HAL) [1] represent widely adopted evaluation techniques designed to assess musculoskeletal disorder risks, specifically focusing on upper body and hand-intensive tasks, respectively. RULA employs observational analysis of joint angles, forces, and postures to generate risk scores indicating the

urgency of ergonomic intervention. The Rapid Entire Body Assessment (REBA) extends this approach to full-body posture evaluation [42]. The NIOSH lifting equation provides quantitative guidelines for manual material handling tasks [117], while the Ovako Working Posture Analysis System (OWAS) offers systematic evaluation of working postures [46]. HAL quantifies ergonomic risk based on task frequency, cycle time, and force requirements, providing threshold limit values for hand-intensive activities. Despite widespread adoption, these traditional assessment methods face limitations including dependence on expert ratings, which are labor-intensive and susceptible to inter-rater variability [121]. Subjective evaluation components in methods like HAL further complicate consistent and standardized assessments across different evaluators and industrial contexts.

Sensor-Based Ergonomic Risk Assessment

The limitations of traditional observational ergonomic assessment methods have driven the development of sensor-based approaches that offer objective, quantitative, and continuous monitoring capabilities. RULA assessment has been adapted for automation through sensor technologies, with systems such as Microsoft Kinect employed to estimate operator poses and conduct non-intrusive ergonomic assessments [72, 23, 37, 90]. More recent advancements have included the use of Kinect v2 sensors for real-time ergonomic assessments and automated RULA scoring, providing cost-effective methods to assess work postures [67]. However, vision-based systems face inherent limitations including occlusions, accuracy issues in dynamic environments, and challenges in tracking complex movements, which reduce the precision and robustness of ergonomic evaluations.

Wearable sensor technologies have emerged as promising alternatives for continuous ergonomic monitoring in manufacturing environments. Inertial measurement units (IMUs) and accelerometers have been extensively investigated for posture and movement analysis [95]. Significant work includes using wearable mobile sensors to analyze postures of construction workers, demonstrating the efficacy of non-invasive monitoring in identifying ergonomic risks [80]. Subsequent research [81] improved this approach with machine learning, allowing

for automated risk monitoring and enhancing the accuracy and scalability of ergonomic assessment. Wearable stretch sensors have been employed to monitor human movement and detect falls, addressing critical safety issues in workplace ergonomics, though challenges such as sensor calibration and false positives remain [13].

Electromyography (EMG) sensors provide direct measurement of muscle activity, offering insights into physical strain and fatigue that are not readily apparent through postural analysis alone. [78] utilized surface EMG sensors with machine learning for ergonomic risk assessment during manual material handling, focusing on muscle activity to evaluate physical strain while acknowledging concerns around sensor comfort and data privacy. Multi-sensor fusion approaches have been developed to combine data from multiple sensor modalities, including IMUs, force sensors, and physiological monitors, to provide comprehensive ergonomic assessment capabilities [112].

Currently, research in hand-intensive manufacturing focuses primarily on the quality of manufactured parts rather than assessing or mitigating the impact on operators performing these tasks [48]. Advances in machine learning have been used to optimize process parameters and predict output quality in various manufacturing processes, such as textile draping and spun-lace production [125, 123, 124, 93]. Yet, very few studies have explored the complex, adaptive motions involved in these manual processes from an ergonomic perspective [38, 28].

Recent developments in machine learning applications to ergonomic assessment have shown significant promise for addressing traditional limitations. A comprehensive review of machine learning in manufacturing ergonomics is provided in [58], which discusses models tailored to individual operators, analysis of operator-workplace interactions, and system-level ergonomic design. Recent approaches include using spatiotemporal convolutional networks for segmenting object manipulation actions to predict ergonomic risks [88] and developing multi-task learning frameworks that simultaneously analyze human activity and ergonomic risk [87]. These advances represent progress toward automated, objective, and scalable ergonomic assessment systems.

Despite these technological advances, several challenges persist in sensor-based ergonomic

assessment. A systematic review on wearable devices in ergonomic applications [101] highlights current limitations, particularly issues of standardization and data quality. Sensor calibration, data synchronization across multiple sensing modalities, battery life, and user acceptance remain significant practical challenges. Furthermore, the translation of sensor data into actionable ergonomic insights requires sophisticated data processing and interpretation algorithms that can account for individual variability and task-specific requirements.

The integration of advanced sensing technologies with machine learning approaches offers substantial potential for transforming ergonomic assessment in manufacturing environments. Real-time monitoring capabilities enable immediate feedback to operators and supervisors, facilitating proactive intervention before injuries occur. Objective measurement reduces reliance on subjective assessments and expert interpretation, improving consistency and reliability of ergonomic evaluations. Continuous data collection enables long-term trend analysis and identification of gradual degradation in ergonomic conditions that might not be apparent through periodic observational assessments.

Nevertheless, achieving greater consistency and accuracy in ergonomic assessment methods remains a significant challenge, necessitating further development of data-driven solutions to address these gaps. While sensor-based ergonomic assessment represents substantial progress in protecting worker health and safety, situations persist where ergonomic improvements are insufficient or economically unfeasible. In such cases, where manual processes present inherent ergonomic risks or involve repetitive, time-intensive operations that contribute to worker fatigue and potential injury, automation of these manufacturing tasks becomes advantageous. The development of adaptive learning systems and intelligent automation technologies offers alternative approaches to address ergonomic challenges while maintaining production efficiency and quality standards.

2.3 Adaptive Learning in Manufacturing and Automation

The limitations of traditional ergonomic interventions and the persistent challenges in manually intensive manufacturing processes have driven the development of adaptive learning

systems and intelligent automation technologies. When ergonomic improvements prove insufficient or economically unfeasible, automation emerges as a viable alternative to reduce human exposure to repetitive, hazardous, or physically demanding tasks while maintaining production efficiency and quality standards. Adaptive learning in manufacturing encompasses the integration of machine learning algorithms, real-time sensor feedback, and intelligent control systems to create manufacturing processes that can automatically adjust to changing conditions, optimize performance, and reduce reliance on human operators in high-risk scenarios.

The evolution of adaptive manufacturing systems has been characterized by the progressive integration of artificial intelligence and machine learning techniques with traditional manufacturing control systems. Early adaptive manufacturing approaches focused on statistical process control and feedback mechanisms [77]. The emergence of Industry 4.0 paradigms has accelerated the development of cyber-physical systems that combine physical manufacturing processes with computational intelligence [56]. These systems enable real-time adaptation to process variations, equipment degradation, and changing production requirements through continuous learning and optimization algorithms.

Machine learning-based adaptive control systems have demonstrated significant capabilities in manufacturing optimization and automation. Reinforcement learning algorithms have been successfully applied to manufacturing process control, enabling systems to learn optimal control policies through interaction with the manufacturing environment [116]. Deep learning approaches have enabled adaptive quality control systems that can automatically adjust process parameters based on real-time product quality measurements [99]. These adaptive systems reduce the need for manual intervention and expert knowledge while improving process consistency and product quality.

Process optimization has been advanced through hybrid approaches combining machine learning with physics-based modeling. [31] developed optimization frameworks combining probabilistic machine learning with finite element analysis for autoclave cure cycles, achieving optimized solutions with reduced computational effort. Similarly, [19] developed physics-

guided neural operators using residual Fourier neural operators for composite curing process modeling, integrating physics priors to predict temperature and cure fields with limited training data. Zero-defect manufacturing approaches have been developed by [115], using homogenization schemes with Gaussian Process Regression to achieve significant improvements in dimensional accuracy. These approaches demonstrate the potential for adaptive learning systems to automate complex manufacturing processes while maintaining high quality standards.

Digital twin technologies have emerged as comprehensive frameworks for manufacturing process control and optimization, representing a paradigm shift toward fully adaptive manufacturing systems. [84] developed frameworks for manufacturing with real-time monitoring, predictive analytics, and closed-loop control systems applied to composite manufacturing processes. [79] advanced machine learning-based process monitoring for automated composites manufacturing, using thermal history data and finite element analysis for automated fiber placement and proposing digital twin development for real-time quality prediction and process control. These digital twin approaches enable automated decision-making and process adaptation without requiring continuous human oversight.

Development of discrepancy models for complex manufacturing systems, using augmentations to finite element models from collected measurement data, exemplifies the integration of adaptive learning with traditional engineering approaches. Digital twin models have become integral to enhancing manufacturing processes, leveraging data-driven and physics-based approaches to improve predictive maintenance, customization, and damage detection. Early work explored the integration of digital twins with predictive maintenance systems, demonstrating their potential in enabling advanced fault detection using physics-based modeling [2, 3]. Expanding this concept, data-driven approaches emerged, highlighting the capability of digital twins to dynamically adapt to real-time sensor inputs for process optimization, as shown in industry use cases for manufacturing efficiency [102]. These advancements laid the foundation for frameworks enabling smart customization and optimization of workflows, combining big data analytics and machine learning for personalized production [114, 65].

The application of adaptive learning systems extends beyond process control to encompass comprehensive manufacturing optimization. Further innovations have been applied to material flow simulation, where physics-based models in digital twins accurately predict bottlenecks and optimize resource allocation [33]. Similarly, additive manufacturing processes have benefited from digital twins integrating physics-based compressive sensing to improve process fidelity and defect detection [61]. For structural applications, hybrid models combining physics-based methods with machine learning have been effectively utilized for damage detection [92]. These applications demonstrate the versatility of adaptive learning approaches in addressing diverse manufacturing challenges while reducing dependence on manual oversight and intervention.

Despite these advancements, several challenges remain in the implementation of adaptive learning systems in manufacturing environments. Data-driven models are often limited by the quality and quantity of training data, potentially leading to inaccuracies in scenarios outside their training set. Physics-based models, while highly precise, are computationally intensive and difficult to scale for large systems or highly stochastic environments. Integrating these approaches requires seamless interaction between data sources and models, a challenge exacerbated by latency, compatibility issues, and cyber-security concerns [2, 33]. Additionally, the transition from manual to automated processes requires careful consideration of safety, reliability, and economic factors to ensure successful implementation.

The convergence of adaptive learning technologies with traditional manufacturing engineering principles represents the most promising approach for addressing contemporary manufacturing challenges. Addressing the limitations of purely data-driven or physics-based approaches requires hybrid methodologies that balance computational efficiency with accuracy while maintaining the interpretability and reliability required for industrial applications. These hybrid approaches combine the predictive capabilities of machine learning with the fundamental understanding provided by physics-based models, resulting in robust and adaptable manufacturing systems.

The development of accurate hybrid models that integrate adaptive learning capabilities

also enables advanced control strategies, including optimal actuator placement and intelligent control system design. Such models provide the foundation for precise control authority distribution and system optimization, allowing for greater control over manufacturing processes while minimizing the number of actuators required and optimizing their placement for maximum effectiveness. This capability becomes particularly important in complex manufacturing systems where precise control of multiple parameters is essential for achieving desired outcomes while maintaining system efficiency and reliability.

2.4 Optimized Actuator Placement

The optimal placement of sensors and actuators has been a fundamental challenge in engineering design for decades, as it directly impacts system performance, control authority, and operational cost. Early foundational work focused on developing methods for placement in large-scale flexible structures by maximizing metrics of controllability and observability [59]. Building upon these principles, later strategies introduced optimization techniques tailored to improve system performance while minimizing costs in specific structural applications [86]. A significant advancement in managing the computational burden of these large-scale systems was the use of balanced reduced models, which provided a systematic approach to maintain system fidelity while reducing model complexity, thereby enabling more efficient solutions [82].

As research progressed into the 2010s, methodologies were adapted to address the dynamics of increasingly interconnected systems and large dynamical networks, optimizing placement for robust control and state estimation across multiple components [104]. A critical theoretical breakthrough occurred when several key controllability metrics were shown to possess submodular properties [103, 108]. This discovery was pivotal, as it provided theoretical guarantees for the performance of efficient greedy algorithms, offering a tractable approach to the otherwise NP-hard problem of minimal actuator placement. This theoretical groundwork paved the way for more sophisticated optimization frameworks, such as the formulation of the placement problem as a mixed-integer semidefinite program to find

globally optimal solutions for both stable and unstable systems [14].

More recently, the field has seen two parallel streams of advancement: the rise of data-driven methods and the development of highly specialized physics-based models. Data-driven approaches emerged that leverage sparsity and known patterns in system dynamics to reduce the number of sensors required for reconstruction tasks without sacrificing accuracy [69]. Concurrently, specialized physics-based methods were developed for specific applications, including techniques based on the Gramian compensability matrix for static load compensation in adaptive beams and plates [113, 50] and the use of topological derivatives to incorporate the shape optimization of actuators into the placement problem [27]. Subsequent work has sought to merge these paradigms, combining data-driven strategies with balanced model reduction to create efficient algorithms that scale effectively with system complexity [71] and extending concepts to cost-constrained sensor selection using dynamically relevant bases [22].

One major trajectory has focused on increasing mathematical rigor and certainty within physics-based paradigms. This path progressed from foundational metric-based approaches [59] toward sophisticated, application-specific formulations for adaptive structures [113, 41] and culminated in powerful frameworks that guarantee global optimality through exhaustive search procedures like branch-and-bound and mixed-integer programming [14, 98]. In contrast, the second trajectory embraced the flexibility and adaptability of data-driven techniques, which excel in scenarios where physical models are incomplete or computationally intractable. This data-centric view, initiated by work leveraging sparsity [69] and later integrated with model reduction [71] or applied to related problems like optimal filtering [105], prioritizes empirical performance and scalability. The work on submodularity [103, 108] can be seen as a bridge between these worlds, providing rigorous theoretical bounds for computationally efficient greedy algorithms that avoid the expense of global optimizers.

Despite the significant progress in both physics-based optimization and data-driven methodologies, persistent challenges related to the trade-offs between computational efficiency and placement accuracy remain, particularly for high-dimensional systems, as does the complex task of integrating physical constraints and uncertainty quantification into placement

strategies [86, 82]. Notably, a significant gap in the literature is the absence of work that holistically integrates adaptive, physics-based modeling with modern data-driven approaches for actuator optimization. This thesis, therefore, focuses on developing robust algorithms capable of bridging this gap by handling uncertainty and leveraging real-time data to adapt to dynamic changes in system behavior, thereby combining the strengths of both established research paradigms.

Chapter 3

MULTIMODAL SENSING TESTBED AND ERGONOMIC RISK SCORE ANALYSIS

3.1 Introduction

This work presents a holistic, data-driven ergonomic assessment framework for hand-intensive manufacturing, particularly focusing on composite layup tasks [1]. Our approach involves multi-modal data collection—including 3D upper body and hand poses, as well as hand force data—combined with ergonomic scoring using industry standards such as RULA and HAL. Additionally, we introduce a novel ergonomic metric, the Biometric Assessment of Complete Hand (BACH), designed specifically to assess hand and finger-level risks. By training machine learning models to predict ergonomic scores based on multi-modal data, we aim to provide a scalable and effective solution for real-time ergonomic assessment, enhancing worker safety and reducing injury risks. The flow of multi-modal data from the sensors to the data processing pipeline for ergonomic score assessment and prediction is shown in Figure 3.1. The specific contributions of this work include:

- An integrated, multi-modal sensor testbed is developed to capture data on operator pose and forces during hand layup process.
- A specialized model is presented that integrates finger and hand movements with upper body pose and hand force data to provide a comprehensive ergonomic assessment. This assessment includes industry-standard RULA and HAL scores, along with a novel BACH score.
- Automated scoring of the existing RULA and HAL risk metrics generalize well to

[1] Approved for Public Release RROI #24-180410-BCA

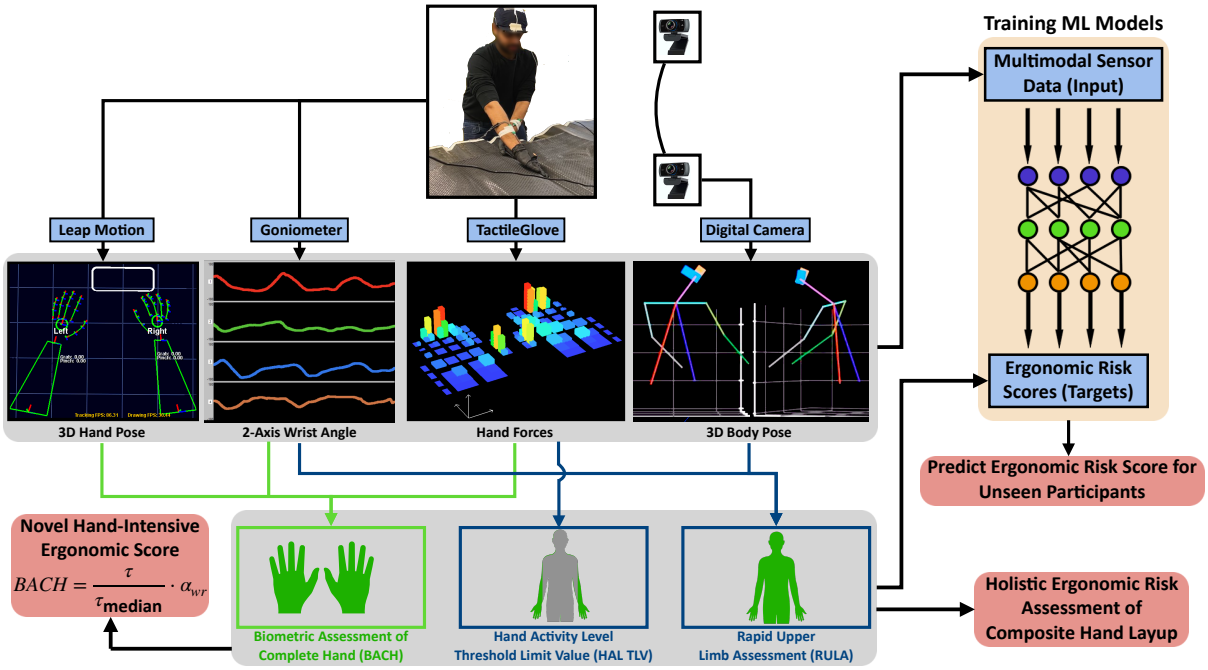

Fig. 3.1 | Data-driven Ergonomic Risk Assessment Pipeline. Multi-modal sensor data from goniometers, Leap Motion, TactileGlove, and webcams are processed through machine learning models to predict RULA and HAL scores, while computing the novel BACH score for comprehensive ergonomic assessment.

unseen participants using machine learning.

- Empirical results show that BACH score captures hand and wrist injury risks at a higher fidelity as compared to the widely-used HAL and RULA scores.

3.2 Data Collection

The selected sensors completely characterize the complex force motion combinations arising in hand-intensive manufacturing processes. Two digital cameras, manufactured by Nexigo (Beaverton, OR, USA), are placed at the front-left and front-right of the operator. These capture the operators' upper body from two distinct perspectives, which is then used to

reconstruct the 3D body pose.

The output from these two cameras is processed using the AlphaPose [29] algorithm. AlphaPose is an advanced deep learning tool designed for human pose estimation, specializing in detecting and mapping human body joints in images and videos. Then, we perform bundle adjustment using a checkerboard pattern to calibrate and concurrently refine the 2D and 3D coordinates of the checkerboard corners together with the corresponding rotation and translation between the two cameras. By combining the 2D joint coordinates from AlphaPose with the rotation and translation of the two webcams, the 3D coordinates of the joints are triangulated, thereby, creating a comprehensive 3D skeletal model of the operator. The remaining sensors capture arm, hand and finger motions and forces.

First, the Ultraleap Stereo IR 170 manufactured by Ultraleap (Mountain View, CA, USA) is used to record 3D hand and arm pose. This sensor records high-fidelity information about the hand and forearm joints using both infrared and visual spectrum cameras and reports 21 three-dimensional coordinates of the skeletal hand pose per hand. Next, wrist motion is captured in two axes using wired electronic goniometers, manufactured by Biometrics Ltd. (Cwmfelinfach, UK). Wrist angle is already reported by the Ultraleap IR 170 by depth sensing of the forearm and hand using infrared cameras. However, consultations with ergonomists and hand layup operators revealed that the wrist experiences the highest loads, and is likely to be the most frequently injured part. Therefore, we use this high-fidelity goniometer to ensure that wrist data are captured accurately and inter-sensor reliability is corroborated. Finger and palm forces are captured using the TactileGlove, manufactured by Pressure Profile Systems (Glasgow, UK), a pair of force-sensing gloves with 65 force-sensing elements per hand. These sensors accurately measure the location and magnitude of the forces applied by the palms and fingers. The complete testbed with all the sensors for data collection is shown to the left in Fig. 3.3.

The layup tools, materials, and shop aides cover the different types of hand motions typically performed by an operator on the factory floor. The two tools used for data collection are shown in Fig. 3.2. The stringer tool is chosen for its multiple concave curvatures along

its length. The operator has to use their fingers or shop aides to ensure that the carbon fiber material accurately conforms to the concave surface by applying concentric pressure to the radii to avoid bridging. In contrast, the convex mold tool is characterized by a large convex curvature. The radius of this curvature varies along the length of the tool, requiring operators to perform smoothening motions that are characteristically almost opposite of those in the stringer tool. We also use two types of materials: a 0/90° plain-weave fabric and unidirectional tape. The material stiffness and forming behavior depend on the direction in which the ply is placed on the tool, each requiring a slightly different layup strategy. Therefore, the fabric is placed at 0° and 45° with respect to the tool, and the unidirectional material is placed at 0° and 90° with respect to the tool.

A total of 15 participants were recruited for data collection[2]. The participants performed

[2]This study complies with all the relevant ethical regulations and is approved by the University of Washington IRB Committee B under ID STUDY00013896. Informed consent was obtained from all the participants prior to their involvement in the study, and participant height, weight, gender, and skill level were self-reported.

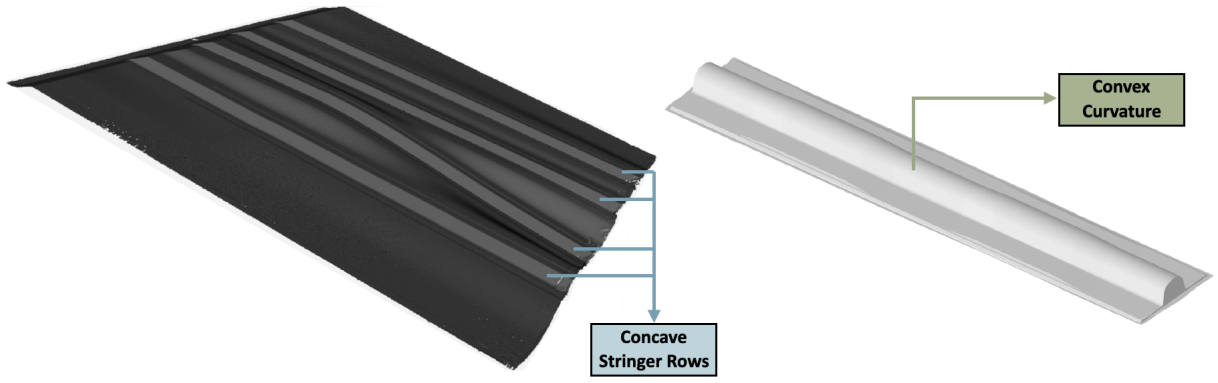

Fig. 3.2 | Digital scans of the two tools used for data collection. 3D scans of the Stringer tool (left) and Convex Mold tool (right) show the difference in geometry between the many concave rows of the Stringer and the convex curvature with varying radii along the length of the Convex Mold Tool.

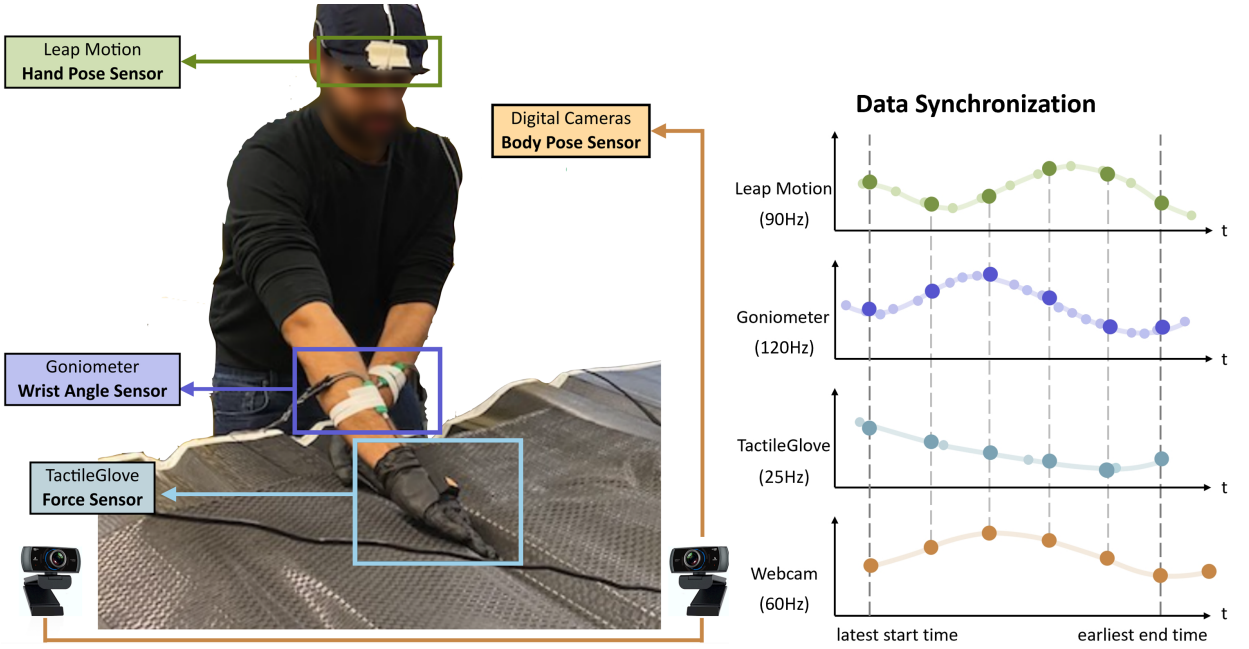

Fig. 3.3 | Data Collection Testbed and Illustration of Data Synchronization. The sensor setup (left) collects data as participants perform composite hand layup, with the Leap motion sensor attached on the helmet, the goniometers attached to both the wrists, the TactileGlove worn on both the hands and two webcams (out of image) capturing stereo images. Sensors with varying frame rates are aligned and synchronized to the frame timing of the webcam (right). The smaller dots represent intrinsic sensing rates and the larger dots represent the interpolated and webcam-aligned data points.

layup for 15 minutes per tool on average. A total of 314 variables were captured at different sensing rates during each trial, which lasted for (5-15) minutes following a standard test procedure. The total data collection time was between (30 - 35) minutes per participant, leading to an overall 7 hours of recorded data. There was significant variation in the height (mean = 169.33 cm, std. dev. = 8.23 cm) and weight (mean = 155.13 lbs., std. dev. = 28.25 lbs) of the participants. The participants' experience level (mean = 4.08 years, std. dev. = 5.54) tended to be either low ($\leq$ 3 years) or high ($\geq$ 10 years). There were 7 female and 8

male participants in this study. Participants were allowed to use two shop aides in selected trials, with the expectation that they would help reduce the stress on the operators' hands and fingers by providing a wide base and a narrow tip to access the grooves.

The large volume and heterogeneity of the collected data, varying measurement rates of the sensors, and occasional sensor failures lead to challenges in sensor synchronization and pre-processing. Prior to initiating the trial, the two portable computers' internal clocks are synchronized with the International Standard Time. Next, a Python script on both the computers is tasked with capturing the start and end times of data collection trials for each sensor separately. A synchronization pipeline then determines the common operational duration across all the sensors and trims their data to this unified time frame. Subsequently, the pipeline interpolates or down-samples sensor data to conform to the digital camera's operational frame rate of 60 frames per second. A schematic of this data synchronization pipeline is shown to the right in Fig. 3.3.

3.3 Existing Ergonomic Assessments for Upper Body and Hand Activity

Ergonomic risk assessment of composite hand layup begins with annotation of the collected data from the operators with existing industry-standard ergonomic scores, namely RULA scores for the upper body and HAL scores for the hands. RULA is a point-based observational analysis of the joint angles and forces sustained by the upper body when executing the motion under evaluation [75]. It has the lowest score when the upper body is in a neutral posture, with penalties for deviations from this posture. The scores increase corresponding to the applied loads and decrease if there is additional support to the legs or arms. The scores for the different parts of the upper body are combined using lookup tables to provide a single score ranging from 1-7.

RULA is calculated for each static posture in the dynamic movements comprising hand layup for each frame of data as follows. First, the 3D coordinates of the various body joints (obtained from AlphaPose) are used to compute the required arm, neck, and trunk positions and angles. Second, the wrist angles (obtained from goniometers) are used to compute the

wrist position and twist. Third, the Muscle Use Score is set to 1 when the action repeats more than 4 times a minute, the Force/Load Score is set to 2 for repeated loads between 4.4 and 22 lbs., and the Leg Score is set to 1 as the legs are supported in hand layup. This information is used in the corresponding lookup tables A, B and C, to calculate the RULA score for a single frame. The entire dataset is annotated frame-by-frame in this manner, thereby generating a time series of RULA scores for every 3D body pose and wrist angle.

The ACGIH developed ergonomic metrics [1] for assessing the risks of work-related distal upper extremity musculoskeletal disorders. The developed metric combines Hand Activity Level (HAL) and Normalized Peak Force (NPF) to estimate the Threshold Limit Value (TLV). HAL is a 10-point score calculated subjectively by experts viewing the performed task. These experts take into account the exertion frequency, rests, and speed of motion according to the specified guidelines. Subsequent efforts [54] developed linear regression models and lookup tables to predict the expert-rated HAL and NPF scores. We use the estimator defined by the nonlinear regression model of Radwin et al. [91]

$$\text{HAL} = 6.56\ \ln\left(\frac{DF^{1.31}}{1+3.18F^{1.31}}\right)\ \text{, where } F = \frac{\text{Exertions}}{\text{Work Time}} \tag{3.1}$$

The duty cycle D is defined as the ratio of work time to the total time, including rest, for a given task. Exertions are typically characterized by the speed of motion and pauses. In composite hand layup, some activities, such as repositioning material on the tool, are less strenuous than applying pressure to the surface. Therefore, exertions are calculated as the time spent above specific force thresholds, detailed below. Since data is collected only during material layup and not during rest periods, we use an average duty cycle of $D = 75\%$, based on operators' responses to a questionnaire about their working and resting times. The working period for exertion calculations is set to the mean layup motion duration, defined as Work Time $= 10\,\text{s}$, based on observations of typical layup activity. Force thresholds are determined using the nominal forces sustained by the flexor digitorum superficialis (FDS) tendon, which facilitates flexion in the metacarpophalangeal and proximal interphalangeal joints of all fingers except the thumb. Typical force values for various hand functions are

provided in Table 5 of [57]. During power grasp activities—comparable, though not identical, to hand layup—the FDS tendon typically sustains forces in the range of 4 N to 20 N. Based on discussions with ergonomists and operators' perceived levels of effort during data collection, two force thresholds are considered: a finger force threshold of 15 N (3.3 lbs) and an overall hand force threshold of 44.8 N (10 lbs). An exertion is recorded when the load on an individual finger exceeds the finger threshold or when the total load on the hand exceeds the overall threshold.

$$\text{Exertions} := \begin{cases} \text{Exertions} + 1 & f_i > \text{Finger Force Threshold} \\ \text{Exertions} + 1 & \sum_{i=1}^{5} f_i > \text{Overall Force Threshold} \end{cases} . \tag{3.2}$$

where,

$$f_i = \text{Sum of forces applied by finger i}$$

The HAL score is, therefore, computed as follows. First, the forces applied over each element in a finger is summed up, and this is repeated for all the five fingers. Next, for the first ten seconds, the number of exertions is counted using equation (3.2). F is computed using Exertions, and subsequently the HAL score using D and equation (3.1). This step is repeated after sliding over the time window by a single data point and annotating the next time window with a corresponding HAL score until the last data point is reached. Therefore, the resultant HAL score is a continuous time-windowed score that is offset from the collected data by 10 seconds. The score is then padded with zeros at the start to ensure it is of the same length as the collected data and consistent with the other ergonomic risk scores.

Figure 3.4 presents histograms of RULA and HAL scores for all the participants, categorized as low risk (green), medium risk (yellow), and high risk (red). RULA scores are classified as low (0-3), medium (4,5), and high (6,7), while HAL scores are categorized as ($0 < HAL < 4$), medium ($4 < HAL < 7$), and high ($HAL > 7$).

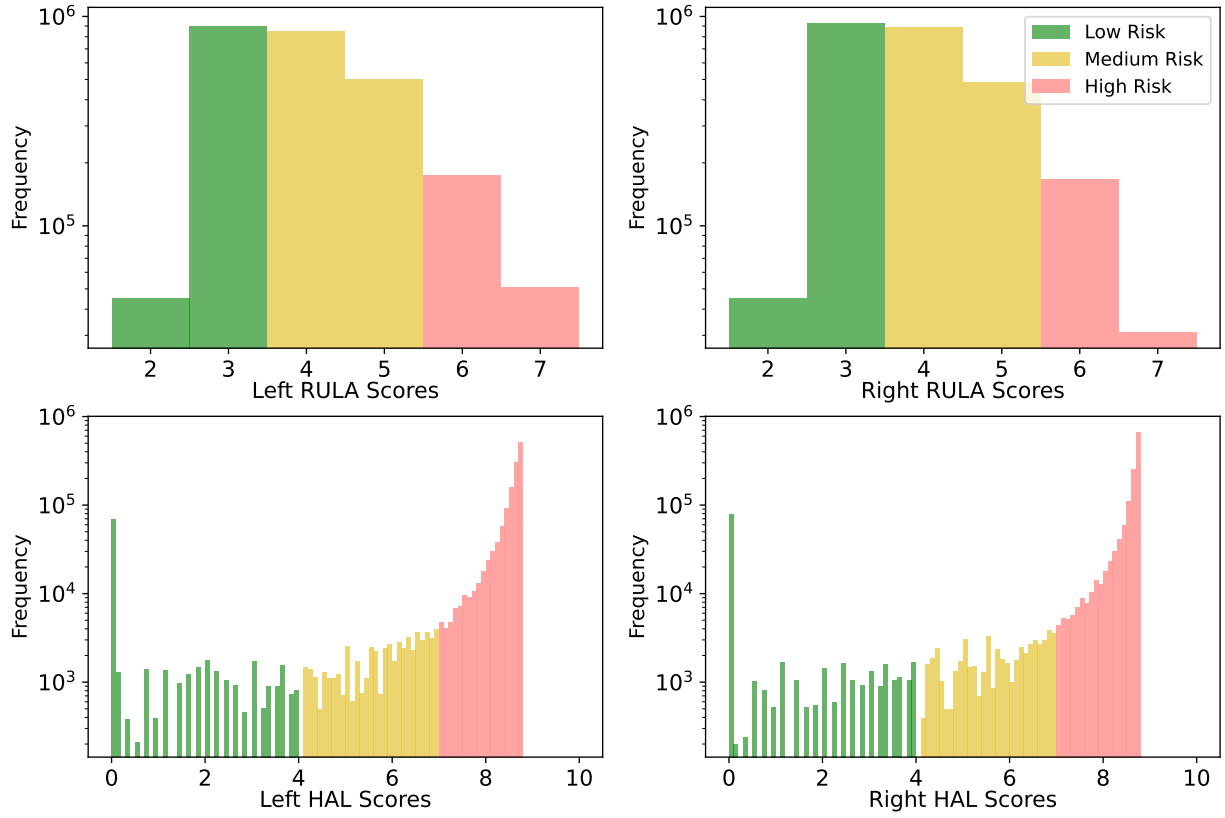

Fig. 3.4 | RULA and HAL Score Distributions. Histograms of RULA and HAL risk scores, categorized as low (green), medium (yellow) and high (red), are presented across all participants, with number of occurrences (frequency) on the y-axis. A significant portion of RULA scores fall in the medium risk range, indicating the need for operators to bend while applying force during layup. However, HAL scores most frequently fall in the high-risk category, highlighting frequent crossing of safe thresholds during composite hand layup.

3.4 New Score for Assessing Hand Motion Risk: BACH

The existing ergonomic risk scoring techniques have a few caveats in their assessment. RULA, for example, is not dynamic, although some adjustments exist for the total forces applied and muscle use. However, the information about the variation and location of these forces is not taken into account. RULA also focuses on the entire upper body, with no special emphasis

on the hands apart from the deviations from the natural wrist position. Therefore, it cannot be used as the only ergonomic assessment of a hand-intensive process, such as hand layup. Even hand-intensive metrics such as HAL TLV need augmentation. The correlation between TLV and injury risk was studied for 908 operators in the cross-sectional assessment in [30], which reported the prevalence of MSDs even at acceptable levels of TLV, suggesting the need for metrics that can better characterize the ergonomic risks in the hands. Informed by research indicating that wrist pressure plays a significant role in hand fatigue, chronic tendon problems, and potential injuries [4, 39], we develop the Biometric Assessment of Complete Hand (BACH) score, which focuses on the effects of hand layup motions in the wrist area.

The BACH score is derived by integrating data from three sensors: the goniometer, Leap Motion sensor, and the TactileGlove. Utilizing the hand pose information from the Leap Motion sensor and both finger and palm force measurements from the tactile glove, the computed force across the hand region is used to determine the resultant torque at the wrist joint. However, the absolute wrist torque may not inherently capture the variability in the individual physiological conditions. Consequently, we propose using the median of the torque as a normalization factor for each subject's torque data. The wrist angle's state directly impacts the tendon dynamics, which, in turn, plays a pivotal role in hand injury risk.

We obtain the relationship between the wrist flexion angle and wrist flexion moment from [44]. As shown in Fig. 3.5, the moment progressively increases when force is applied in the positive flexion direction as the wrist transitions from extension to flexion. It reaches its peak at approximately 40°and subsequently begins to decline. This observation implies that the maximum applicable flexion moment is constrained by the biomechanical characteristics of the hand. Consequently, it serves as an indicative parameter for assessing wrist safety during force application. Specifically, a higher achievable wrist moment at a given wrist angle corresponds to a reduced injury risk. As an extension of this principle, the inverse wrist moment at the corresponding wrist angle can be employed as a multiplicative factor for the normalized torque.

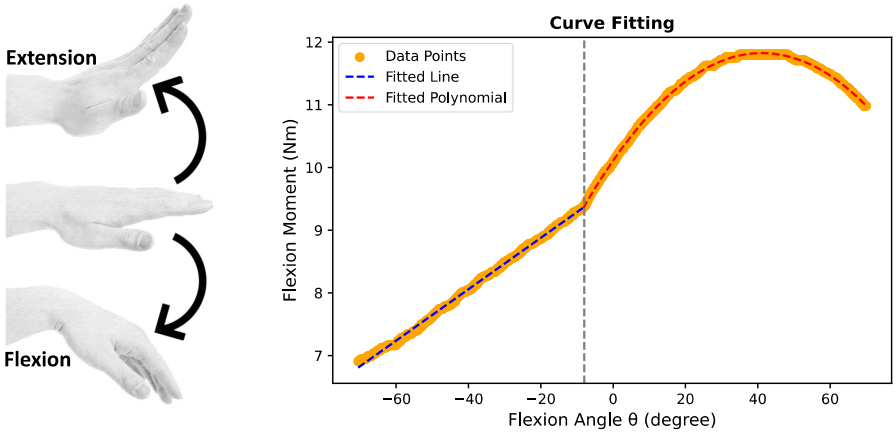

Fig. 3.5 | Hand poses illustration (left) and maximum isometric wrist flexor/extensor moments vs. flexion angle (right) during positive flexion force [44]. The curve comprises two segments: a linear relationship in the left section and a quadratic relationship in the right section, fitted using linear and second-degree polynomial models respectively.

We define the BACH score as a function of the ratio of wrist torques τ over the median of wrist torque τ_{median} and a multiplicative scaling factor α_{wr}, characterized by the ratio of the maximum wrist flexion moment, $\max_\theta M_{\text{flex}}(\theta)$, to the flexion moment of a given wrist angle θ, $M_{\text{flex}}(\theta)$.

$$\text{BACH} = \frac{\tau}{\tau_{\text{median}}} \cdot \alpha_{\text{wr}} \tag{3.3}$$

where

$$\alpha_{\text{wr}} = \frac{\max_\theta M_{\text{flex}}(\theta)}{M_{\text{flex}}(\theta)} \tag{3.4}$$

$$M_{\text{flex}}(\theta) = \begin{cases} 0.041\theta + 9.696, & \text{for } -90^\circ < \theta \leq -8^\circ \\ -0.001\theta^2 + 0.083\theta + 10.110, & \text{for } -8^\circ < \theta < 90^\circ \end{cases} \tag{3.5}$$

The parameters for the piecewise function $M_{\text{flex}}(\theta)$ are derived using curve fitting on the graphical data presented in [44].

3.5 Hand-Focused Ergonomic Risk Analysis

To assess the applicability of our BACH score, we first plot the variations in the wrist angles and torques for all the seven participants, separately for their right and left hands, in Fig. 3.6. We observe consistent trends in the right and left wrist torques among the participants, which highlight their individual strength disparities. To determine which hand exhibits higher torque values, we applied the Mann-Whitney U test [68]. The null hypotheses was H_0: "The two torque distributions are identical", and the alternate hypothesis was H_1: "The right-hand torque distribution is greater than the left-hand distribution". The test was conducted on $N = 1.4 \times 10^6$ samples, yielding $U = 1.07 \times 10^{12}$, $p = 7.7 \times 10^{-132}$, confirming a significantly higher occurrence of elevated torque values in the right wrists as compared to the left wrists. This result aligns with the right-handed dominance observed in all the study participants. Additionally, the wrist angles show differences in how the left and right hands are positioned, indicating that the two hands play different roles during hand layup tasks. We then select four representative sections from the hand layup trials to illustrate the characteristic patterns in the RULA, HAL, and BACH assessments. These sections portray the temporal alignment of the three distinct evaluation metrics, providing a more comprehensive visual assessment of the subjects' hand layup movements.

In Fig. 3.7, the top section illustrates a progression from gentle material rubbing with low metric scores to material pinching, resulting in higher wrist torques. As the operator leans forward using wrist support, RULA reaches high risk while BACH drops due to force alignment through the wrist. The final stages show sustained HAL elevation despite decreasing finger force, concluding with two-handed pressing that peaks BACH scores. Throughout, RULA fluctuates with posture changes while HAL maintains stable trends due to its computational parameters. BACH provides more detailed real-time assessment, complementing HAL's limited temporal resolution. In the bottom section, the operator begins with repetitive pinching motions to conform material to the curved tool surface, causing oscillations in the BACH score. The process then shifts to fingertip smoothing at the tool's edge, reducing

force and lowering BACH scores. Increased finger pressing afterward raises the BACH score to a moderate level. Next, edge manipulation with the fingertips reduces the palm-force angle and shortens the wrist torque lever arm, lowering BACH scores. HAL then shows a delayed response to the decrease in hand activity intensity, attributed to its thresholding and windowing computation method. Throughout these activities, RULA remains at medium risk levels due to stable upper-body posture.

The top section of Fig. 3.8 demonstrates a dynamic sequence of hand activities: BACH score initially fluctuates with repetitive pressing, then significantly drops during hand surface smoothing in the second frame. The score rises again as the operator employs fingertip precision for narrow groove fitting, followed by increased whole-hand pressure for material

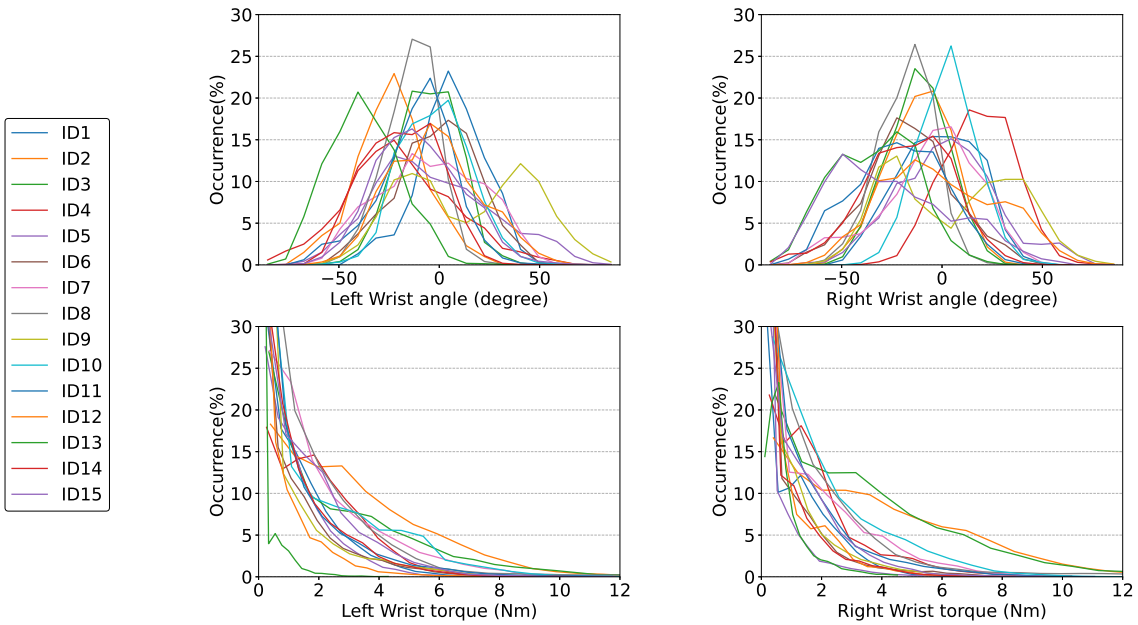

Fig. 3.6 | Wrist angle and torque distributions for all the participants during hand layup tests. The wrist torque patterns emphasize right-handed dominance for the participants. The variations in the wrist angles suggest different roles for the left and right hands during hand layup.

conformity. BACH peaks in the final frame when the operator leans forward, channeling body weight through hand pressure. Throughout these transitions, HAL demonstrates a consistent pattern of delayed response to decreasing movement intensity, while RULA variations specifically track the operator's forward-leaning postures and their associated risks. The bottom section exhibits a distinct progression of hand movements: starting with minimal wrist torque during left-hand material holding, then transitioning to precise fingertip manipulation in narrow grooves. This is followed by whole-hand pressure application with added body weight, before shifting to lower-intensity thumb-dominant pressing. The sequence concludes with a return to material holding motion to support right-hand layup activities. As in the top section, HAL shows delayed responses to two distinct decreases in movement intensity, while RULA scores correspond directly to changes in upper body weight engagement throughout the layup process.

Visualizations of the two layup sections highlight the utility of the RULA score for assessing overall body posture risk, while the HAL and BACH metrics provide a more detailed focus on hand region analysis. Although the HAL score captures hand activity over extended timeframes, it lacks the precision for immediate, detailed hand risk assessment. The BACH score addresses this limitation, offering a more robust and nuanced evaluation of hand risk. Consequently, it adds an alternative dimension that could significantly enhance hand risk monitoring.

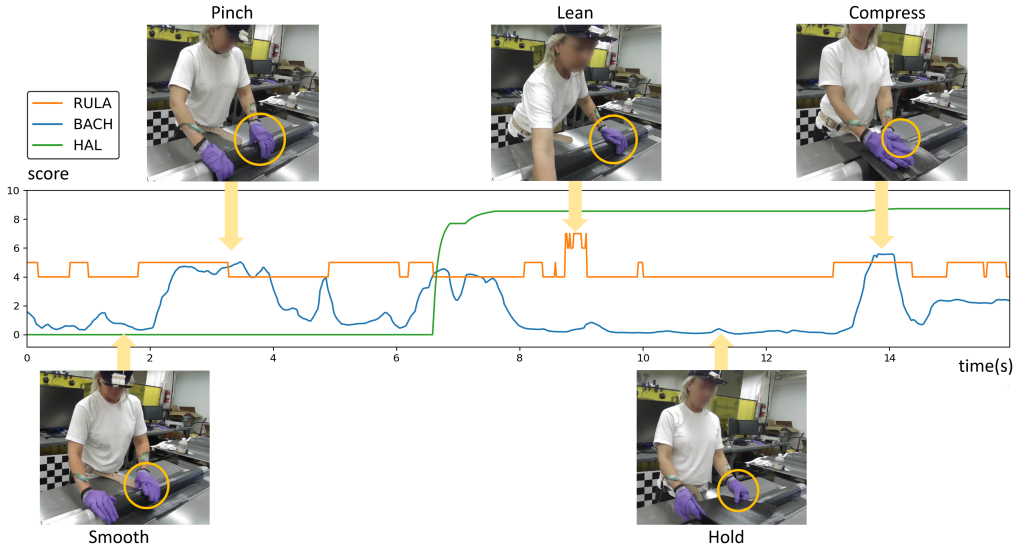

(a) BACH progresses from low scores during initial layup to peaks during pinching. RULA rises with poor posture mid-task, while BACH drops during material placement before rising again with final conforming force, and HAL shows delayed risk responses to hand activity.

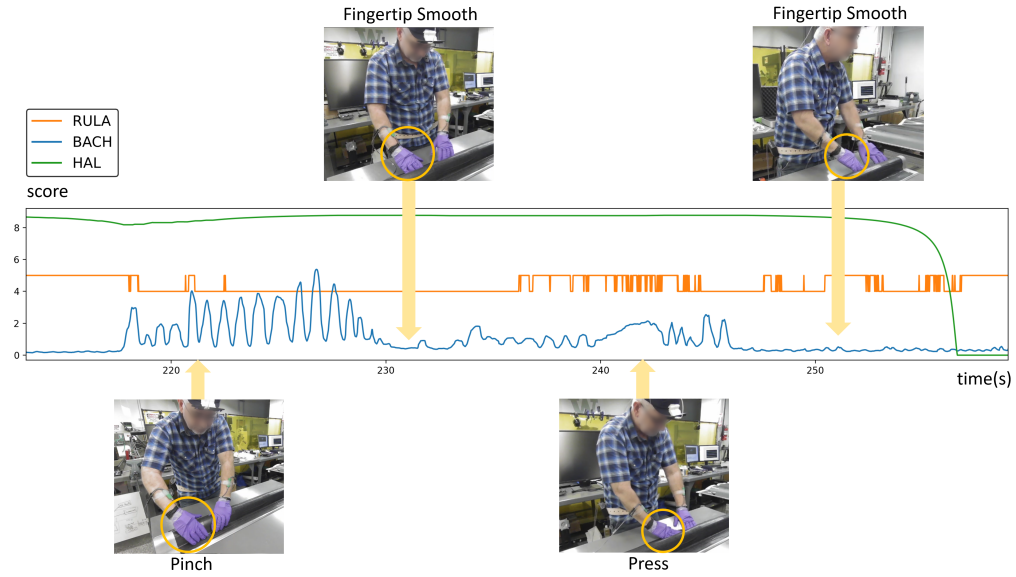

(b) BACH score fluctuates: high during pinching, low during smoothing, rising with pressing, then decreasing with return to smoothing, RULA maintains medium risk with minor fluctuations and HAL score exhibits an offset delayed response.

Fig. 3.7 | Comparative Analysis of Hand Motion-Based Ergonomic Scores. RULA, HAL, and BACH scores are shown from two selected trials along with the corresponding frames of interest from the digital camera.

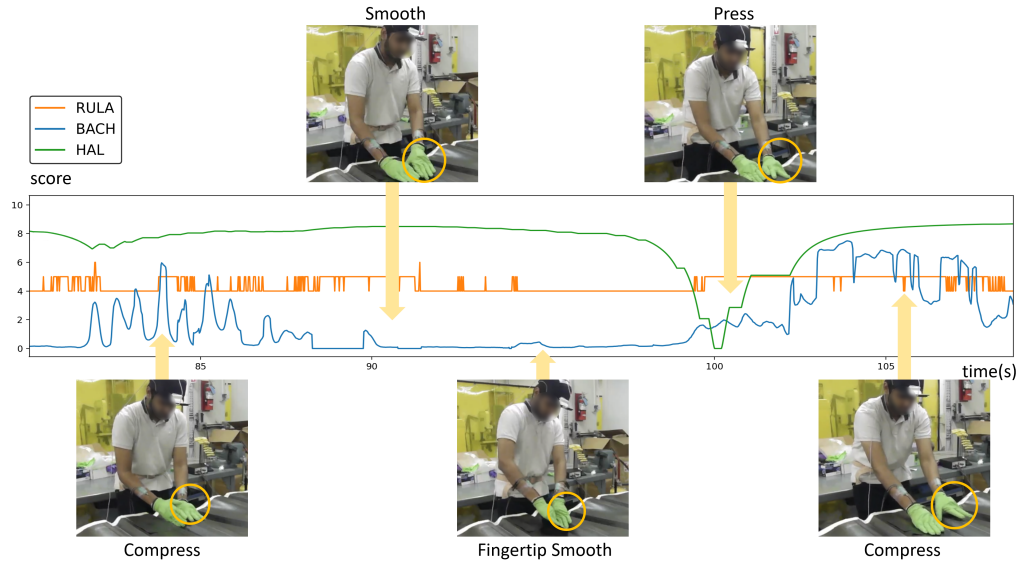

(a) BACH score fluctuates through task sequence: high during pressing, low during smoothing, rising with fingertip work, increasing with whole-hand pressure, and peaking with forward-leaning body weight application.

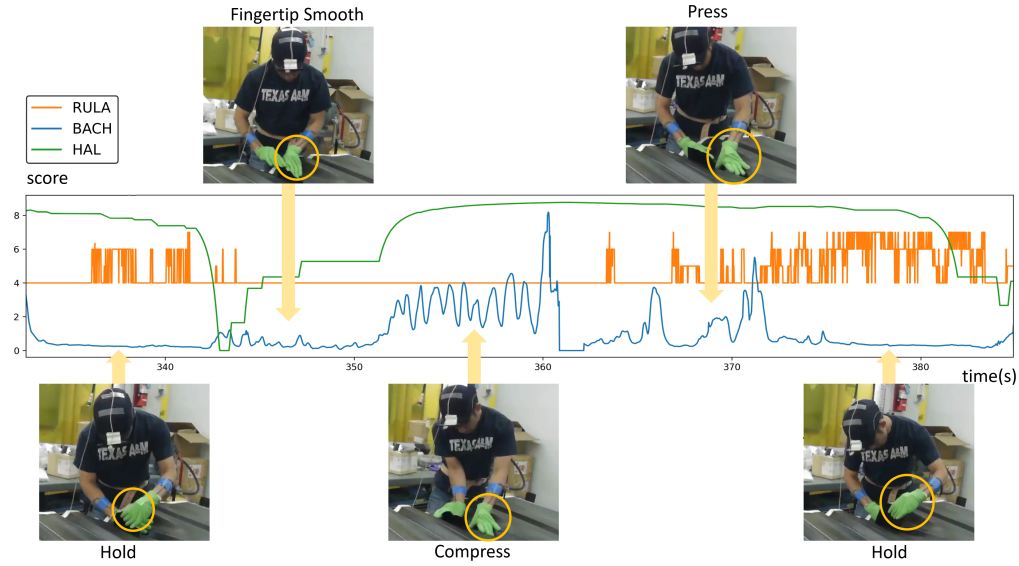

(b) Task progresses from minimal wrist torque during material holding, to fingertip precision work, then whole-hand pressure, before shifting to lighter thumb pressing and final pinching motion. HAL shows delayed response to movement intensity, while RULA reflects upper body engagement.

Fig. 3.8 | Additional Comparative Analysis of Hand Motion-Based Ergonomic Scores. RULA, HAL, and BACH scores are shown from two selected trials along with the corresponding frames of interest from the digital camera.

Chapter 4

MACHINE LEARNING MODELS FOR PREDICTING ERGONOMIC RISK IN UNSEEN PARTICIPANTS

4.1 Machine Learning Models

Machine learning (ML) models are selected based on the similarity of the modeling technique to the risk scoring mechanism. Decision trees consist of branches that assign outputs y based on optimized thresholds (β) of the feature (x) values in the data

$$\begin{cases} y \leftarrow y_1 & \text{if } x < \beta \\ y \leftarrow y_2 & \text{if } x \geq \beta \end{cases}. \tag{4.1}$$

Here, the desired output is the RULA risk score, and x are the upper-body posture and joint angles, therefore the decision tree mimics the incrementation of RULA scores based on predetermined threshold of joint angles. In doing so, decision trees mimic the complex RULA lookup table, but also offer more interpretability of the specific force-motion combinations directly affecting risk. We use a gradient boosted classifier, which uses ensembles of decision trees to predict risk. Specifically, gradient boosted classifiers train a sequence of decision trees, starting with a simple decision tree with high bias and low variance. Sequentially, more complex decision trees with lower bias and higher variance are added, resulting in models which are less prone to overfitting while having adequate complexity. At each nth stage of training, a new estimator $h_n(x)$ is added to minimize the residual error, $y - y^*$, between the output of the current model, $y = F_n(x)$, and the true risk, y^*, as follows

$$F_{n+1}(x) = F_n(x) + h_n(x) = y^* \tag{4.2}$$

When designing the predictors for HAL, the model needs to account for it being a time windowed score that uses a history of hand force inputs. Recurrent Neural Networks (RNN)

use a hidden layer that is updated with each force input, and, therefore, has a memory that can capture the temporal dynamics of the input forces. We train Gated Recurrent Units (GRUs), a type of RNN [21], which can handle longer input sequences than RNNs with traditional activation functions such as the hyperbolic tangent. GRUs, along with Long-Short-Term Memory (LSTM) [43] networks use gating mechanisms to map sequential force inputs to outputs (HAL score). Update gates $\mathbf{z}$ and Reset gates $\mathbf{r}$ control the flow of information from the past to the future and are computed by applying σ, the logistic sigmoid activation function, elementwise to weighted input and previous hidden states. The weights are then updated to minimize the difference between the predicted and true HAL score.

$$\mathbf{r} = \sigma(\mathbf{W}_r\mathbf{x} + \mathbf{U}_r\mathbf{h}_{t-1}), \tag{4.3a}$$

$$\mathbf{z} = \sigma(\mathbf{W}_z\mathbf{x} + \mathbf{U}_z\mathbf{h}_{t-1}), \tag{4.3b}$$

where $\mathbf{x}$ is the input state, $\mathbf{h}_{t-1}$ is the previous hidden state, and $\mathbf{W}$ and $\mathbf{U}$ are weight matrices which are learned. Hidden states are computed via elementwise multiplication ($\odot$) of the update gates with previous hidden states

$$\mathbf{h}_t = \mathbf{z} \odot \mathbf{h}_{t-1} + (\mathbf{1} - \mathbf{z}) \odot \hat{\mathbf{h}}_t, \tag{4.4a}$$

$$\hat{\mathbf{h}}_t = \phi(\mathbf{W}\mathbf{x} + \mathbf{U}(\mathbf{r} \odot \mathbf{h}_{t-1})). \tag{4.4b}$$

Here, ϕ refers to the hyperbolic tangent function. The reset gate controls how much information to forget, and the previous hidden state is ignored if $\mathbf{r}$ is near zero. The update gate controls how much information to carry over, and serves to update the hidden unit as a ratio of the previous hidden state $\mathbf{h}_{t-1}$ and the new hidden state $\hat{\mathbf{h}}_t$. GRUs lack context vectors or output gates like LSTMs, but have been shown to have similar performance while being simpler to compute and train [21]. The reader is referred to section 4.3 for implementation details of the GRU and gradient boosting classifier models.

4.2 Generalization of RULA and HAL Scores to Unseen Participants

Automated RULA and HAL scoring from sensor data is evaluated using holdout validation, where data from one participant is reserved for testing while the model is trained on data from the remaining participants. This approach assesses the model's ability to generalize and learn force-motion patterns associated with ergonomic risk in unseen participants. Data collection was performed using two tools with representative geometries: convex (Stringer) and concave. As all participants were right-handed, results are split by tool geometry and the hand in use to highlight any differences in scoring performance across these conditions, and shown in Fig. 4.1.

We categorize risk levels into three classes: low, medium, and high. This classification facilitates comparisons between HAL (0–10 scale) and RULA (1–7 scale) scores and provides practical recommendations from numerical values. To ensure conservative risk estimation, correct classifications are combined with predictions that are one class higher than the true risk level (e.g., low classified as medium, or medium classified as high). This approach promotes recommendations for ergonomic changes even in marginal cases. Fig. 4.1 shows the percentage of data for each test participant which is correctly or conservatively classified (green), incorrectly classified by one class (low), and incorrectly classified by two classes (red) for RULA and HAL. Tables 4.1 and 4.2 provide the actual and predicted RULA and HAL risk levels as percentages of the collected data for all participants.

The RULA predictor achieves over 95% classification accuracy for nearly all participants, across both hands and tools, demonstrating its ability to model new technicians' behavior by learning correlations between sensor data and RULA scores. The figure also reveals atypical behavior on Participant 1, Participant 11 (left and right) and Participant 12 (left) with the Stringer tool. This anomaly is primarily caused by partial occlusion of the lower section of the upper body in the camera setup, leading to inaccuracies in estimating hip position using AlphaPose and, consequently, imprecise upper body leaning angle measurements. Additionally, feature importance analysis (Supplementary Table 3) reveals that the upper extremities

of the upper body are the most critical predictors of risk.

The HAL predictor achieves over 95% classification accuracy for nearly all participants across both hands and tools. Notably, accuracy is higher for the left hand than the right, with atypical values observed in Participants 11–13 and, to a lesser extent, Participants 9 and 15 on the Stringer tool. Investigation revealed that force sensors on the TactileGlove saturated near the tip of the dominant (right) hand due to high local pressure, leading to incorrect force data. The GRU model, trained on these correlations, mapped the saturated data to excessively high HAL scores. When force sensor data does not saturate, the HAL predictor generalizes well, maintaining excellent accuracy across most holdout participants. In contrast, the RULA predictor shows fewer two-class misclassifications, likely due to its simpler scoring model based on angle and load thresholds, as opposed to the nonlinear functions and windowed frequency measurements used in HAL. Classification performance drops are primarily due to occlusion or sensor force saturation. Additional trials could improve holdout performance by increasing population variance and optimizing sensor configurations.

4.3 Details of ML models

Gated Recurrent Units (GRUs) [20], a type of Recurrent Neural Network (RNN), are used to predict our time-dependent HAL score, which is implemented in Pytorch. The reset gate r_t, update gate z_t, new gate n_t, and the candidate hidden state h_t are computed componentwise as follows (equivalent to Equations (8-9) in the main text

$$
\begin{aligned}
r_t &= \sigma(x_t W_{ir} + h_{t-1} W_{hr} + b_r) \\
z_t &= \sigma(x_t W_{iz} + h_{t-1} W_{hz} + b_z) \\
n_t &= \tanh(W_{in} x_t + b_{in} + r_t \odot (W_{hn} h_{t-1} + b_{hn})) \\
h_t &= (1 - z_t) \odot n_t + z_t \odot h_{t-1}
\end{aligned}
$$

where x_t is the input at time t, $h_{t-1}$is the hidden state at time $t-1$ or the initial hidden state at $t = 0$. σ is the sigmoid function, and $\odot$ denotes the Hadamard product. The W and b terms denote the weight matrices and biases respectively, which are updated iteratively to

improve prediction performance. We use a multilayer GRU, therefore the input $x_t^{(l)}$ of the l-th layer ($l \geq 2$) is the hidden state $h_{t-1}^{(l-1)}$ of the previous layer.

The model was also developed in Python 3.11, using PyTorch and PyTorch Lightning developed for GPU hardware accelerators and an Nvidia-CUDA compatible laptop with an RTX 4080 GPU. Here are the salient features of the model, identified after searching over possible structures and hyperparameters via grid search.

- **Structure:** Sequentially, the first layer is a Gated Recurrent Unit (*torch.nn.GRU*) with $(input\_size, hidden\_size, num\_layers)$ = (6,10,3), with 6 inputs referring to the instantaneous force on the five fingers and the palm section. This is followed by a dense layer (*torch.nn.Linear*) with $(in\_features, out\_features)$ = (10,90), followed by another dense layer (*torch.nn.Linear*) with $(in\_features, out\_features)$ = (90,1) which produces HAL as output.

- **Optimizer and Loss Function:** The ADAM optimizer [49] (*torch.optim.Adam*) is used with a learning rate, $lr = 1e-3$. Huber Loss is used as our Loss Function (*torch.nn.HuberLoss*) with $(delta, reduction)$ = (1,'mean').

- **Training and Early Stopping:** This model is trained for a maximum of 25 epochs with a batch size of 1024. The increased batch size resulted in a significant increase in accuracy, suggesting that the increased variance of bigger batches can more accurately capture force trends corresponding to HAL scores. We have also implemented Early Stopping (*pytorch_lightning_callbacks.EarlyStopping*) with $(monitor, patience)$ = $(train\_loss, 3)$. This moves the model from inference to training when the training loss hasn't improved in the last 3 epochs, resulting in less overfitting to the training data.

The Gradient Boosting Classifier is a state-of-the-art classifying technique that uses multiple weak learners to produce a prediction. This technique produced the best results when trained using the angles formed by the upper body as input and the corresponding RULA

scores as output. This model was developed in Python 3.11 and uses the Sklearn and XGBoost packages. XGBoost is used for GPU-based hardware acceleration during training, and its Sklearn API is used to interface with Sklearn's functions for hyperparameter optimization and model selection. The hyperparameters were tuned initially over the entire parameter space with a randomized search, and fine-tuned with a grid search. All except one participant's data is used for training, with the results being demonstrated on the held out participant, similar to the GRU model. We note that the cameras are able to see more of the technician in the Convex Mold Tool compared to the Stringer Tool, due to the smaller size of the tool. Here are the details of this model.

- **Structure:** We used a pipeline (*sklearn.pipeline.Pipeline*) of a standard scaler (*sklearn.preprocessing.StandardScaler*), and a gradient boosting classifier (*xgboost.XGBClassifier* with (tree_method,sampling_method) = ('gpu_hist','gradient_based').

- **Hyperparameters and Loss:** We set (n_estimators,max_depth,learning_rate,gamma, min_ child_weight,max_leaves) = (29,6,0.018,0.12,1,27) after performing an extensive coarse and fine grid search. We use the F1 score (*sklearn.metrics.f1_score*) as the loss function.

4.4 Additional Results

This section has the detailed risk level results for the HAL and RULA predictors respectively. Table 4.1 shows the RULA model holdout validation accuracy in percentage. The risk levels are segmented as low, medium and high based on the risk levels, namely, low (0-3), medium (4,5), and high (6,7). Table 4.2 shows the HAL model holdout validation accuracy in percentage. We use three classes for the risk levels, namely, low ($0 < HAL < 4$), medium ($4 < HAL < 7$), and high ($HAL > 7$). The results have been split based on the left and right hand, and also based on the tools. The results mainly show the classifier generalizes well to new participants.

Table 4.3 shows the ranking of the most important features for a RULA classifier trained on the 3D body coordinates. This table thus shows the most important features the classifier uses to predict the RULA score, ranked using the Maximum Relevance Minimum Redundancy algorithm [89]. The L, R, or Mid designations refer to the left or right side of the body, or their average respectively. Channels 1 and 2 of the goniometer represent flexion and extension angles of the wrist. This table highlights the importance of the upper extremities in determining risk, namely, the shoulder and elbow positions, along with the wrist flexion/extension angle.

4.5 Discussion

Our sensor-driven ergonomic scoring framework is of immediate applicability in numerous common manufacturing tasks involving human grasp, pressure and smoothing. The developed BACH score in particular, quantifies hand and digit activity in granular detail not afforded by other metrics (HAL and RULA). Given the prevalence of dexterous activity in manufacturing and the need for safe, efficient automation of repetitive tasks, this framework opens several promising directions for future work. Data-driven and learning-based approaches can further characterize the biomechanics of dexterous hand movements, particularly by linking hand pose and activity with indicators of tendon injury. In addition to data-driven risk scoring, such ML approaches can learn improved models of existing risk metrics such as HAL, including learning nonlinear models directly from data [10, 97], optimizing model or measurement parameters to extract maximal information [70] or to generalize to specialized hand activities. Additionally, feature engineering of pose-force combinations can inform the development of assistive robotics, exoskeletons, and partial automation for dexterous processes. Automated decision-making in such systems could be enhanced by incorporating information on local geometry, material properties, and user-preferred movement patterns.

Notably, shop aides were not used consistently across the trials, particularly by less experienced participants. As a result, they did not significantly reduce the participants' RULA,

HAL, or BACH scores. However, the use of shop aides did impact task completion times. For the tasks where the operators utilized the shop aides over 50% of the duration, completion times were compared against those completed without any aide. A Mann-Whitney U-test was applied with the null hypotheses H_0: "The two completion times are identical", and the alternate hypothesis H_1: "Completion times without the shop aide are greater than those with the shop aide". Conducted on $N = 15$ samples, the test yielded $U = 179.5$, $p = 0.003$, indicating that shop aides significantly reduced the task completion times while maintaining comparable layup quality, thereby, mitigating prolonged exposure to high ergonomic risks. Nevertheless, we plan to redesign the shop aides using the BACH score and the wrist torque metric to encourage the operators to use the thumb to apply the same force instead of other fingers. This is expected to result in a lesser overall wrist torque for the same applied force, as the thumb is closer to the wrist than the other fingers. The thumb, being the topmost finger when applying force downwards, helps maintain the forearm in a neutral position, which has been shown to minimize ergonomic risks as compared to other non-neutral positions [76].

Building on these observations, we can further refine ergonomic interventions by optimizing operator techniques and workplace setups. Targeted ergonomic adjustments can be made to both operator techniques and workplace setup in tasks like composite hand layup to lower injury risk. First, modifications to operator movements and force application are recommended, based on trials demonstrating that low-risk movements and reduced force achieve the same layup quality with less injury potential. Secondly, adjustments to the workplace, informed by analysis of upper body postures, can facilitate safe access to tool extremities without significantly raising RULA scores. By examining tool mounting angles and access points, this ergonomic assessment can also help improve the operator's baseline posture during composite hand layup tasks.

Data collection and model training for this study were conducted using two laptop computers, integrating both sensors and computational capabilities to create a fully portable ergonomic risk assessment testbed. Our goal is to use this tool to assess ergonomic risks associated with hand-intensive activities across both manufacturing and non-manufacturing

settings. The real-time inference and risk scores generated by these ML models provide technicians with immediate feedback on the most ergonomically hazardous aspects of their tasks. This feedback enables targeted adjustments—either through workplace modifications, enhanced access to the tool, expert guidance on safer techniques, or the design of shop aides that reduce exposure time and improve reach to challenging areas.

While this portable tool shows promise for real-time ergonomic risk assessment in diverse work environments, challenges remain in achieving fully reliable data. Issues like sensor saturation, missing measurements, and connectivity disruptions underscore the need for robust data handling methods to ensure model accuracy and comprehensive ergonomic insights. These failure modes pose challenges in training the most generalizable ML models, as well as in computing BACH scores that capture all the hand activity risks. In the future, it would be useful to investigate suitable data imputation techniques [47] to fill in the missing measurements. Correlation analysis and decomposition methods such as Robust PCA [12] and Dynamic Mode Decomposition [96] can help impute missing data using correlated measurements from other sensors. These techniques also provide dimensionality-reduced representations of complex force-motion combinations, which can be useful for process control and automation.

Addressing these data reliability issues will support the broader goal of developing a comprehensive and objective ergonomic risk assessment. This approach represents an important step toward establishing robust injury metrics that help understand how and why operator injuries occur in manufacturing settings. By shifting from subjective, expert-based assessments to sensor-driven, objective evaluations, we can minimize errors associated with inter-rater reliability and improve accessibility. Accurately predicting injury risk remains challenging due to factors such as cumulative physical and mental fatigue. A truly comprehensive assessment will require integrating a broader range of measurable variables during evaluation.

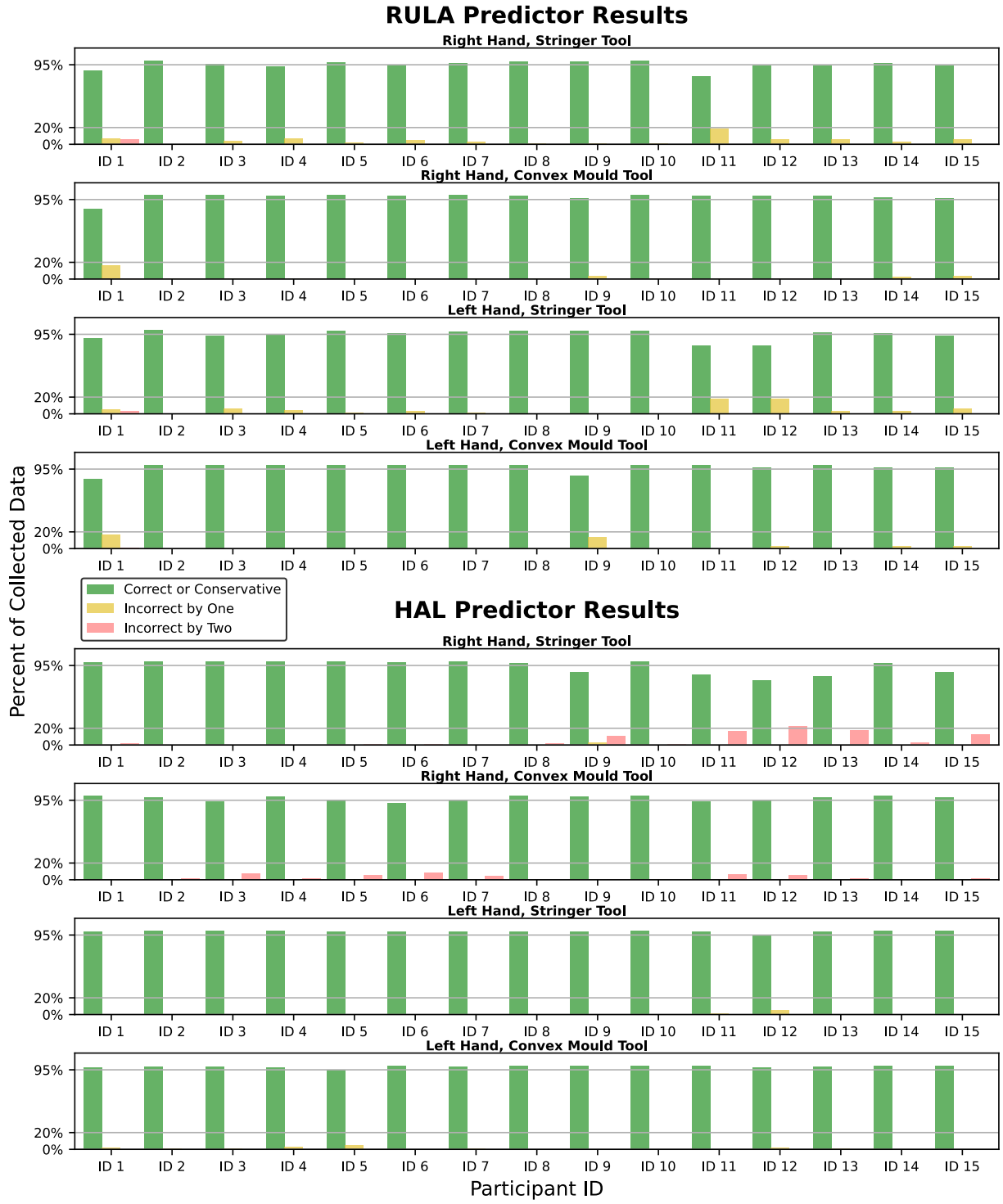

Fig. 4.1 | RULA and HAL Prediction Results. Both the HAL and RULA predictors achieve over 95% classification accuracy for almost all the participants, across both the hands and tools. Instances of misclassification are primarily attributed to sensor malfunctions.

Right,Stringer Tool Participant ID	Correctly Classified	True=Low Predicted=Medium	True=Low Predicted=High	True=Medium Predicted=High	True=Medium Predicted=Low	True=High Predicted=Medium	True = High Predicted=Low
1	81.31	1.45	0.82	4.86	6.08	0.79	4.7
2	99.52	0.1	0	0.03	0.12	0.23	0
3	93.7	0	0	2.09	0	4.21	0
4	91.94	0.96	0	0.51	0.33	6.22	0.05
5	96.69	0.86	0	0.73	0.12	1.61	0.01
6	91.6	0.58	0.12	2.51	0.93	4.24	0.02
7	96.07	0.14	0	0.75	0.05	2.96	0.03
8	90.94	0	0	7.53	0.08	1.43	0.01
9	95.07	0.03	0	4.15	0.01	0.74	0
10	98.92	0.05	0	0.37	0	0.66	0
11	78.03	0	0	3.5	0	18.47	0
12	88.51	0	0	5.22	0	6.27	0
13	93.42	0	0	0.41	0	6.17	0
14	95.91	0.15	0	0.92	0.13	2.88	0.01
15	93.56	0	0	0.19	0	6.25	0
Right,Convex Mold Tool Participant ID	Correctly Classified	True=Low Predicted=Medium	True=Low Predicted=High	True=Medium Predicted=High	True=Medium Predicted=Low	True=High Predicted=Medium	True = High Predicted=Low
1	82.55	1.34	0.02	0.12	15.69	0.05	0.23
2	99.96	0	0	0	0	0.04	0
3	99.67	0.12	0	0	0.01	0.2	0
4	97.97	1.06	0	0.01	0.53	0.38	0.04
5	99.82	0.09	0	0	0.01	0.08	0
6	98.41	0.65	0	0.05	0.5	0.4	0
7	99.89	0.09	0	0	0.01	0.01	0
8	98.16	1.55	0	0	0.26	0.02	0.02
9	94.76	0	0	1.49	0	3.75	0
10	99.72	0	0	0.08	0.03	0.17	0
11	97.8	1.55	0	0.28	0.18	0.18	0
12	98.91	0.18	0	0	0.17	0.73	0.01
13	90.17	0	0	9.42	0	0.42	0
14	95.26	1.76	0	0.35	0.3	2.32	0
15	96.03	0	0	0.58	0	3.38	0
Left,Stringer Tool Participant ID	Correctly Classified	True=Low Predicted=Medium	True=Low Predicted=High	True=Medium Predicted=High	True=Medium Predicted=Low	True=High Predicted=Medium	True = High Predicted=Low
1	84.8	1.64	2.17	4.49	5.07	0.77	1.07
2	99.63	0.14	0	0.02	0.05	0.15	0
3	91.22	0	0	2.28	0	6.5	0
4	94.28	0.94	0	0.52	0.34	3.91	0.02
5	96.03	1.33	0	1.42	0.07	1.14	0
6	92.59	1.33	0.01	2.17	0.5	3.3	0.11
7	97.43	0.14	0	0.54	0.01	1.84	0.04
8	87.07	0	0	11.99	0.04	0.85	0.05
9	95.1	0.04	0	4.03	0	0.82	0
10	98.87	0.04	0	0.47	0	0.62	0
11	75.68	0	0	5.87	0	18.45	0
12	79.21	0	0	2.37	0	18.43	0
13	81.29	0	0	15.69	0	3.02	0
14	95.9	0.11	0	0.7	0.1	3.16	0.03
15	93.45	0.01	0	0.06	0	6.48	0
Left,Convex Mold Tool Participant ID	Correctly Classified	True=Low Predicted=Medium	True=Low Predicted=High	True=Medium Predicted=High	True=Medium Predicted=Low	True=High Predicted=Medium	True = High Predicted=Low
1	81.44	1.45	0.34	0.21	16.24	0.01	0.3
2	100	0	0	0	0	0	0
3	99.75	0.1	0	0.01	0	0.13	0
4	97.85	1.56	0	0.11	0.34	0.09	0.05
5	99.64	0.1	0	0	0	0.26	0
6	98.22	1.19	0	0.06	0.2	0.33	0
7	99.48	0.11	0	0.13	0	0.27	0
8	97.94	1.71	0	0	0.17	0.09	0.09
9	74.42	0	0	12.27	0	13.31	0
10	99.68	0	0	0.16	0.03	0.13	0
11	97.33	1.84	0	0.35	0.11	0.37	0
12	96.89	0.23	0	0.19	0.26	2.41	0.01
13	92.94	0	0	6.74	0	0.32	0
14	95.18	1.84	0	0.23	0.26	2.49	0
15	96.09	0	0	1.06	0	2.84	0

Table 4.1: **RULA Model Holdout Validation Accuracy.** Table showing prediction accuracy of the best performing RULA model (in percent) using XGBoost architecture using holdout validation. The results are the predictions of the model when given the previously unseen sensor data of the current participant while the remaining participants' data and RULA scores are used to train the model. The results are displayed for the right and left hands for both tools used in data collection.

Right,Stringer Tool Participant ID	Correctly Classified	True=Low Predicted=Medium	True=Low Predicted=High	True=Medium Predicted=High	True=Medium Predicted=Low	True=High Predicted=Medium	True = High Predicted=Low
1	97.79	0	1.79	0.41	0	0	0
2	99.98	0	0.02	0	0	0	0
3	99.97	0	0.03	0	0	0	0
4	98.64	0.03	0.17	1.16	0	0	0
5	98.9	0.34	0.55	0.21	0	0	0
6	96.79	0.12	1.14	1.94	0	0	0
7	99.38	0	0.08	0.54	0	0	0
8	96.48	0	1.93	1.59	0	0	0
9	60.05	2.91	10.89	23.56	0	2.59	0
10	97.23	1.15	0.53	1.09	0	0	0
11	82.74	0	16.25	1.01	0	0	0
12	56.93	0.13	22.87	20.08	0	0	0
13	65.73	0	17.64	16.63	0	0	0
14	96.43	0.08	2.66	0.83	0	0	0
15	77.25	0	13.03	9.72	0	0	0
Right,Convex Mold Tool Participant ID	Correctly Classified	True=Low Predicted=Medium	True=Low Predicted=High	True=Medium Predicted=High	True=Medium Predicted=Low	True=High Predicted=Medium	True = High Predicted=Low
1	99.77	0	0.01	0.22	0	0	0
2	96.56	0	1.45	1.99	0	0	0
3	87.55	0.34	7.07	5.04	0	0	0
4	98.14	0	1.16	0.7	0	0	0
5	86.07	2.08	5.6	5.72	0.39	0.14	0
6	82.01	2.47	8.68	6.84	0	0	0
7	94.71	0	4.22	1.07	0	0	0
8	99.23	0	0	0.77	0	0	0
9	97.58	0.15	0.74	1.53	0	0	0
10	97.87	0.41	0	1.67	0	0.05	0
11	90.16	0.59	6.38	2.87	0	0	0
12	91.52	0	5.74	2.74	0	0	0
13	93.07	0.15	1.81	4.97	0	0	0
14	99.6	0.16	0.15	0.09	0	0	0
15	96.53	0.65	1.51	1.3	0	0	0
Left,Stringer Tool Participant ID	Correctly Classified	True=Low Predicted=Medium	True=Low Predicted=High	True=Medium Predicted=High	True=Medium Predicted=Low	True=High Predicted=Medium	True = High Predicted=Low
1	99.55	0.06	0.01	0.02	0.02	0.34	0
2	99.98	0	0.02	0	0	0	0
3	99.97	0	0.03	0	0	0	0
4	99.94	0	0	0	0.01	0.04	0
5	99.22	0	0	0.01	0.07	0.7	0
6	99.45	0.02	0	0	0.48	0.05	0
7	99.45	0.01	0	0	0.06	0.48	0
8	98.97	0.05	0	0.5	0.01	0.47	0
9	92.78	2.31	0.15	4.61	0	0.15	0
10	99.8	0.11	0	0.06	0	0.03	0
11	97.86	1.07	0	0.01	0.49	0.57	0
12	94.6	0.02	0	0.03	0.73	4.62	0
13	97.74	0.19	0.1	1.23	0.64	0.1	0
14	99.29	0.07	0	0.63	0	0.01	0
15	97.56	1.41	0	0.93	0	0.1	0
Left,Convex Mold Tool Participant ID	Correctly Classified	True=Low Predicted=Medium	True=Low Predicted=High	True=Medium Predicted=High	True=Medium Predicted=Low	True=High Predicted=Medium	True = High Predicted=Low
1	96.97	0.06	0.01	0.79	1.16	1.01	0
2	98.68	0.15	0.01	0.08	0.12	0.96	0
3	97.74	0.81	0.01	0.16	0.11	1.17	0
4	97.36	0	0	0	0.76	1.87	0
5	94.86	0.06	0	0.17	2.32	2.52	0.07
6	99.08	0.07	0	0.67	0.01	0.17	0
7	98.6	0.19	0	0.02	0.11	1.07	0
8	99.71	0	0	0.29	0	0	0
9	96.47	0.24	0	2.93	0.3	0.06	0
10	98.75	0.08	0	0.9	0.08	0.19	0
11	97.71	0.67	0.35	1.11	0.01	0.14	0
12	96.56	0.29	0	1.28	0.82	1.05	0
13	94.79	0.64	0	3.25	0.7	0.61	0
14	98.87	0.46	0	0.44	0.01	0.22	0
15	99.85	0.09	0	0.04	0	0.01	0

Table 4.2: **HAL Model Holdout Validation Accuracy.** Table showing prediction accuracy of the best performing HAL model (in percent) using GRU architecture using holdout validation. The results are the predictions of the model when given the previously unseen sensor data of the current participant while the remaining participants' data and HAL scores are used to train the model. The results are displayed for the right and left hands for both tools used in data collection.

Left RULA	Right RULA
Mid_Shoulder - Y	L_Shoulder - Y
L_Gonio - 1	R_Elbow - Z
L_Elbow - X	Mid_Shoulder - Y
L_Eye - Z	R_Elbow - X
R_Shoulder - Y	R_Gonio - 1
L_Shoulder - Y	L_eye - Z

Table 4.3: **RULA Classifier Feature Importance Ranking** Table showing the ranking of features by importance to the RULA scores, ranked using the MRMR algorithm [89]. This classifier used the 3D coordinates of body pose, and the goniometer data. It highlights the importance of shoulder position, wrist flexion/extension angle (given by L_Gonio - 1 and R_Gonio - 1) and elbow angle.

Chapter 5

TOWARDS OPTIMIZING MANUFACTURING IN SMALL AND LARGE SCALE ASSEMBLY

5.1 Validation and Deployment of Ergonomic Assessment

5.1.1 BACH Score Validation and Industrial Applications

The Biometric Assessment of Complete Hand (BACH) score developed in Chapter 3 represents a significant advancement in hand-intensive ergonomic assessment, providing real-time, objective measurement of wrist torque relative to biomechanical capacity. While the BACH score demonstrates superior sensitivity to hand and finger risks compared to traditional RULA and HAL metrics, its validation within the controlled laboratory environment establishes the foundation for broader industrial applications rather than definitive injury prediction.

The BACH score's primary strength lies in its ability to identify ergonomic risk patterns that complement existing assessment methods. When used in conjunction with RULA and HAL scores, BACH enables comprehensive risk assessment that captures both postural deviations and hand-specific biomechanical stresses. This multi-metric approach supports conservative risk estimation, promoting ergonomic interventions even in marginal cases where traditional metrics might not indicate immediate concern. The real-time nature of BACH scoring provides immediate feedback capabilities that are essential for proactive workplace safety management.

The demonstrated effectiveness of BACH in differentiating between high-risk and low-risk hand movements creates opportunities for evidence-based workplace optimization. Manufacturing environments can leverage BACH scores to identify specific tasks, tools, or techniques that contribute disproportionately to ergonomic risk, enabling targeted interventions that

address root causes rather than symptoms. Furthermore, the objective, sensor-based nature of BACH assessment reduces dependence on subjective expert evaluations, improving consistency and scalability across diverse manufacturing environments.

5.1.2 Shop Aide Redesign Using BACH Optimization

Current shop aides employed in composite hand layup processes, while functional for material manipulation, exhibit inadequate ergonomic considerations that could reduce operator risk. Analysis of collected ergonomic data indicates opportunities for tool redesign that would significantly improve BACH scores while maintaining or enhancing manufacturing quality. The BACH scoring framework provides a quantitative optimization objective for systematic tool improvement.

The shop aide redesign process leverages BACH scoring as a design optimization objective, incorporating wrist torque calculations, force distribution analysis, and ergonomic constraint satisfaction to identify tool geometries that minimize operator risk while maintaining task effectiveness. Finite element analysis of tool stress distributions ensures that ergonomic improvements do not compromise tool durability or performance. Material selection considers both ergonomic factors, such as surface texture and thermal properties, and manufacturing requirements including chemical resistance and dimensional stability.

Prototype validation using the established multimodal sensor testbed enables quantitative assessment of ergonomic improvements. Comparative analyses comparing RULA, HAL, and BACH scores between traditional tools and optimized designs across multiple operators and manufacturing scenarios will ensure that optimized designs result in lesser ergonomic risk overall. Task completion time analysis ensures that ergonomic improvements do not negatively impact manufacturing efficiency or quality, creating a comprehensive framework for tool optimization that balances worker safety with operational performance.

5.1.3 Technology Readiness and Industrial Deployment

The ergonomic risk assessment framework developed in Chapters 3 and 4 demonstrates successful proof-of-concept for automated RULA and HAL scoring using multimodal sensor data. Advancing the technology readiness level (TRL) from laboratory demonstration (TRL 4-5) to a deployable product suitable for industrial environments (TRL 7-8) requires addressing key technical and practical challenges while maintaining the accuracy demonstrated in controlled laboratory settings.

The current system architecture, built around portable sensor components including the Ultraleap Stereo IR 170, electronic goniometers, TactileGlove force sensors, and stereo cameras, provides a foundation for industrial deployment. However, transitioning to a finished product necessitates enhanced robustness, standardized interfaces, and streamlined data processing pipelines. The system must operate reliably in diverse manufacturing environments while preserving the multimodal data integration capabilities that enable comprehensive ergonomic assessment.

The envisioned deployment architecture consists of a continuous monitoring system where operators are equipped with the multimodal sensor suite during routine manufacturing tasks. Real-time data streams from all sensors are processed through trained machine learning models to generate instantaneous RULA, HAL, and BACH risk scores. The system architecture includes automated quality checks to identify sensor malfunctions, missing measurements, or connectivity disruptions that could compromise assessment accuracy.

Upon detecting elevated ergonomic risk scores, the system provides immediate feedback to operators and supervisors through visual and auditory alerts. Recommendations are generated automatically based on specific risk factors identified, including suggestions for posture modifications, workplace adjustments, tool redesign, or task rotation. The recommendation engine leverages detailed sensor data to provide targeted interventions, such as suggesting specific wrist angle adjustments or recommending alternative gripping strategies.

A critical component of the deployed system is the implementation of adaptive learn-

ing capabilities that enable continuous model improvement through operational data. As workers use the system during routine manufacturing tasks, high-quality sensor data that passes automated quality checks is incorporated into the training dataset. This continuous data ingestion allows machine learning models to adapt to new operators, evolving manufacturing processes, and previously unseen ergonomic scenarios. Online learning algorithms update model parameters incrementally without requiring complete retraining, while transfer learning techniques enable rapid adaptation to new manufacturing environments or worker populations while preserving fundamental ergonomic relationships learned from the original dataset.

5.2 From Human Factors to Automation

The transition from human-centered ergonomic assessment to manufacturing automation represents a fundamental shift in addressing the challenges of modern composite manufacturing. While ergonomic interventions can reduce worker injury risk, certain manufacturing processes present inherent biomechanical challenges that cannot be fully mitigated through workplace modifications alone. In such cases, automation emerges as an effective long-term solution for eliminating worker exposure to high-risk activities while maintaining or improving manufacturing quality and efficiency.

5.2.1 Ergonomic Risk as a Driver for Manufacturing Automation

Composite hand layup exemplifies a manufacturing process where ergonomic risks necessitate automation consideration. The multimodal dataset collected in this work reveals the extent of biomechanical stress experienced by operators during composite layup tasks. The predominance of high HAL scores observed across participants, combined with elevated BACH scores during critical layup operations, demonstrates that composite hand layup inherently involves force and motion combinations that exceed safe ergonomic thresholds. These findings align with industry reports of musculoskeletal disorders among composite manufacturing workers, particularly those involving repetitive wrist and hand motions.

The repetitive strain associated with composite hand layup presents a compelling case for automation. Unlike ergonomic risks that can be mitigated through workplace redesign or tool modification, the fundamental requirements of composite layup—precise force application, complex hand motions, and sustained awkward postures—create unavoidable biomechanical stress. The temporal analysis of RULA, HAL, and BACH scores throughout layup operations reveals that risk exposure is not limited to specific tasks but is distributed throughout the entire process, making comprehensive ergonomic intervention extremely challenging.

Furthermore, the precision requirements of aerospace composite manufacturing demand consistent force application and motion control that approaches or exceeds human capabilities. The variability observed in operator techniques, while demonstrating human adaptability, also introduces quality control challenges that automation can address. By eliminating human exposure to ergonomic risks while simultaneously improving manufacturing consistency, automation represents a dual solution to both safety and quality concerns in composite manufacturing.

5.2.2 Data-Driven Insights for Automation System Design

The multimodal dataset collected for ergonomic assessment provides valuable insights into the biomechanics of skilled composite layup operations. This dataset, comprising synchronized measurements of upper body pose, hand pose, applied forces, and temporal dynamics, represents a comprehensive characterization of composite hand layup operations. The integration of force measurements with kinematic data enables detailed analysis of the force-motion relationships that define successful layup operations.

Analysis of the collected data reveals distinct motion patterns employed by experienced technicians that differ from those of novice operators. Experienced technicians demonstrate more efficient force application strategies, reduced wrist deviation during critical operations, and optimized hand positioning that minimizes biomechanical stress while maintaining layup quality. These insights provide direct input for automation system design, particularly in the development of end effectors that can replicate the most effective human techniques while

avoiding ergonomically problematic motions.

The force distribution data collected through the TactileGlove sensors offers particularly valuable information for robotic end effector design. The spatial and temporal patterns of force application during material smoothing, conforming, and finishing operations provide specifications for gripper design, force control algorithms, and tool path planning. Additionally, the correlation between hand pose and applied forces enables the development of adaptive control strategies that adjust force application based on material response and geometric constraints.

The dataset's inclusion of both successful and problematic layup techniques enables automation systems to avoid motion patterns associated with high ergonomic risk while incorporating strategies that experienced operators use to achieve high-quality results. This data-driven approach to automation design ensures that robotic systems can match or exceed human performance while eliminating the ergonomic risks that necessitate automation.

5.2.3 Scaling from Hand-Intensive to Large-Scale Manufacturing Automation

While the automation of hand-intensive processes like composite layup addresses local ergonomic and quality concerns, large-scale manufacturing automation presents fundamentally different challenges that require sophisticated physics-informed modeling approaches. The transition from human-scale manipulation to structural-scale control represents a shift from discrete task automation to system-level manufacturing optimization.

Large-scale composite manufacturing involves the manipulation and control of flexible structures that exhibit complex mechanical behavior under loading and environmental conditions. Unlike the localized force-motion relationships characteristic of hand layup, large-scale automation must account for distributed structural responses, boundary condition variations, and material property uncertainties that significantly impact manufacturing outcomes. These challenges are particularly pronounced in aerospace manufacturing, where dimensional tolerances and structural requirements demand precision that exceeds the capabilities of conventional modeling approaches.

Traditional finite element models (FEM), while providing theoretical understanding of structural response, often exhibit significant discrepancies when compared to experimental measurements due to material property variations, boundary condition uncertainties, and unmodeled dynamics. These discrepancies become critical limitations in automated manufacturing systems that require precise prediction of structural behavior to achieve specified dimensional and quality targets.

The challenge of large-scale automation thus extends beyond replicating human motions to developing predictive models that can account for the complex interactions between manufacturing processes and structural responses. This requirement drives the need for hybrid modeling approaches that combine physics-based understanding with experimental data to achieve the prediction accuracy necessary for automated manufacturing control.

5.2.4 Bridging Human Factors and Structural Control

The connection between human factors engineering and large-scale structural control lies in their shared requirement for data-driven optimization of complex manufacturing processes. Just as ergonomic assessment benefits from multimodal sensor integration and machine learning analysis, large-scale manufacturing automation requires the integration of physics-based models with experimental measurements to achieve reliable process control.

The methodological approaches developed for ergonomic assessment—including sensor fusion, uncertainty quantification, and adaptive learning—provide a foundation for addressing the modeling challenges inherent in large-scale automation. The same principles of combining multiple data sources to achieve robust system characterization apply to both human motion analysis and structural behavior prediction.

Furthermore, both domains require real-time decision-making capabilities that balance multiple competing objectives. Ergonomic assessment systems must balance risk minimization with productivity maintenance, while large-scale automation systems must balance dimensional accuracy with manufacturing efficiency. The optimization frameworks and machine learning approaches developed for ergonomic applications provide methodological

precedents for addressing similar trade-offs in structural control applications.

This convergence of methodological requirements motivates the development of integrated approaches to manufacturing optimization that address both human factors and system-level performance considerations. The following sections present a framework for large-scale manufacturing automation that leverages data-driven modeling approaches to achieve the precision and reliability required for advanced composite manufacturing while eliminating the ergonomic risks that drive automation needs.

5.3 Physics-Informed Models for Manufacturing Control

The integration of data-driven methodologies with traditional physics-based modeling has emerged as a critical approach for addressing complex control challenges in manufacturing systems. As highlighted in the literature review, while digital twin technologies and adaptive learning systems show significant promise for manufacturing optimization, persistent challenges remain in bridging the gap between computational models and physical reality, particularly for high-dimensional flexible structures where precise control is essential.

5.3.1 Motivation

Traditional finite element models (FEM), while providing fundamental understanding of structural behavior, often exhibit discrepancies when compared to experimental measurements due to modeling assumptions, material property variations, and boundary condition uncertainties. As noted by Du et al. [26], optimal actuator placement for composite structure shape control remains challenging due to the complex relationship between actuation forces and resulting deformations. Similarly, Yue et al. [122] demonstrated that active learning approaches can address uncertainties in shape control applications, but emphasized the need for robust discrepancy modeling frameworks that can account for model inadequacies.

The literature review revealed that while digital twin approaches have been developed for material flow simulation and additive manufacturing processes, there remains a significant gap in holistically integrating adaptive, physics-based modeling with modern data-driven

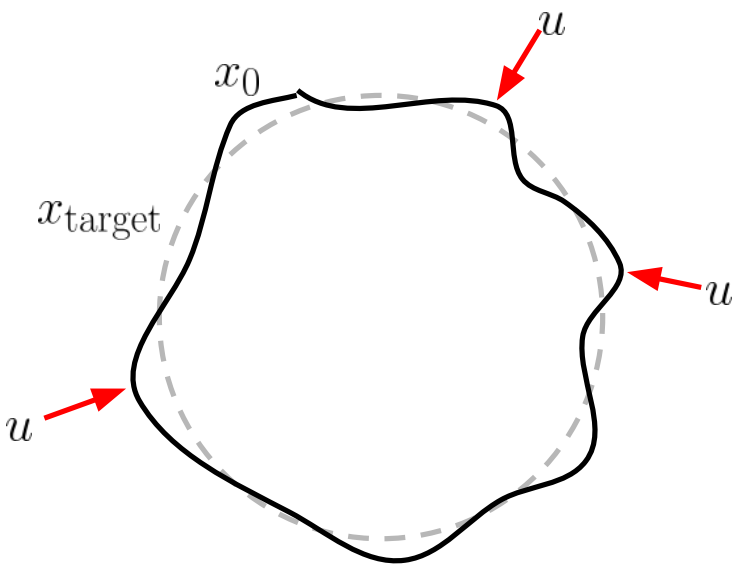

Fig. 5.1 | Flexible structure shape control problem Schematic diagram showing initial configuration x_0, target shape x_{target}, and distributed actuator forces u.

approaches for actuator optimization in flexible structures. Current approaches often rely on either purely physics-based optimization or data-driven methods in isolation, limiting their effectiveness in handling uncertainty and leveraging real-time adaptation capabilities.

5.3.2 Problem Statement

Consider a flexible structure that deviates from its target shape x_{target} due to external loading or manufacturing variations, as illustrated in Figure 5.1. The control objective is to determine optimal actuator locations and forces u to achieve the desired shape transformation from initial configuration x_0 to the target configuration. The shape control problem for flexible structures encompasses three fundamental challenges that must be addressed simultaneously.

First, significant discrepancies exist between physics-based finite element model (FEM)

predictions and experimental measurements, arising from unmodeled dynamics, uncertainties in material properties, and variations in boundary conditions. These model inadequacies can lead to substantial errors in predicted structural responses, necessitating correction through experimental data. Second, the determination of optimal actuator placement requires identifying both the minimum number of actuators and their spatial distribution to achieve specified shape adjustments while maximizing system controllability. This optimization problem is inherently complex due to the high-dimensional nature of the structural response and the discrete combinatorial nature of placement decisions. Third, the integration of experimental measurements with physics-based models demands robust uncertainty quantification methods that can provide reliable confidence bounds on predictions, accounting for both random uncertainties inherent in measurements and systematic uncertainties in model structure.

5.4 Finite Element and Discrepancy Modeling

To address the modeling challenges identified for large-scale manufacturing automation, this section presents the development of a hybrid physics-data approach that combines finite element modeling with experimental discrepancy correction. The approach begins with establishing a baseline finite element model of the flexible structure, followed by systematic correction using experimental measurements to achieve the prediction accuracy required for manufacturing control.

5.4.1 Finite Element Model Development

A finite element model is developed in MATLAB to simulate the deformation and stiffness analysis of a cylindrical composite structure representative of large-scale manufacturing components. The model incorporates material properties and geometric parameters specific to carbon fiber composite materials commonly used in aerospace manufacturing applications.

Property	**Value**
Young's Modulus (E)	7.18×10^6 psi (Carbon)
Thickness Range ($h_{\min}$, $h_{\max}$)	$h_{\min} = 0.215\,\text{in},\ h_{\max} = 0.425\,\text{in}$
Radius and Height (R, b)	$R = 42.65\,\text{in},\ b = 18\,\text{in}$

Table 5.1: **Material properties for the Finite Element model**

Material Properties

Model Geometry and Discretization

The structure is discretized into $N = 414$ beam elements with three degrees of freedom (DOF) per node:

$$\text{DOF} = \{u, v, \theta\}.$$

The element length L_e is given by:

$$L_e = \frac{2\pi R}{N}.$$

Node positions are calculated using polar coordinates:

$$\rho = R + \text{shape\_frequency},$$

where `shape_frequency` incorporates user-defined deformation parameters that enable modeling of manufacturing-induced geometric variations.

Element Stiffness Matrix

The local stiffness matrix for each element is computed using standard beam element formulation:

$$\mathrm{K}_{i,i+1} = \begin{bmatrix} \frac{EA}{L} & 0 & 0 & -\frac{EA}{L} & 0 & 0 \\ 0 & \frac{12EI}{L^3} & \frac{6EI}{L^2} & 0 & -\frac{12EI}{L^3} & \frac{6EI}{L^2} \\ 0 & \frac{6EI}{L^2} & \frac{4EI}{L} & 0 & -\frac{6EI}{L^2} & \frac{2EI}{L} \\ -\frac{EA}{L} & 0 & 0 & \frac{EA}{L} & 0 & 0 \\ 0 & -\frac{12EI}{L^3} & -\frac{6EI}{L^2} & 0 & \frac{12EI}{L^3} & -\frac{6EI}{L^2} \\ 0 & \frac{6EI}{L^2} & \frac{2EI}{L} & 0 & -\frac{6EI}{L^2} & \frac{4EI}{L} \end{bmatrix} \begin{bmatrix} u_1 \\ v_1 \\ \theta_1 \\ u_2 \\ v_2 \\ \theta_2 \end{bmatrix},$$

where E is Young's modulus, A is the cross-sectional area, L is the element length, and I is the second moment of area.

Global Assembly and Boundary Conditions

The global stiffness matrix K is assembled by transforming and integrating the local matrices into the global coordinate system:

$$\mathrm{K} = \begin{bmatrix} \mathrm{K}_{1,2} & 0 & \cdots & 0 \\ 0 & \mathrm{K}_{2,3} & \cdots & 0 \\ \vdots & \vdots & \ddots & \vdots \\ 0 & 0 & \cdots & \mathrm{K}_{n-1,n} \end{bmatrix}.$$

Boundary conditions are applied to represent typical manufacturing fixtures, with specific nodes fixed to simulate clamping and support conditions. Applied forces are specified normal to the surface at actuator locations:

$$\mathrm{f}_{\text{applied}} = \{f_x, f_y, m\}.$$

The finite element model provides predicted deflections under specified boundary conditions and applied loads. Figure 5.2 shows the predicted deflection of the structure under loading, with boundary conditions corresponding to nodes 413 and 414 fixed to represent typical manufacturing constraints.

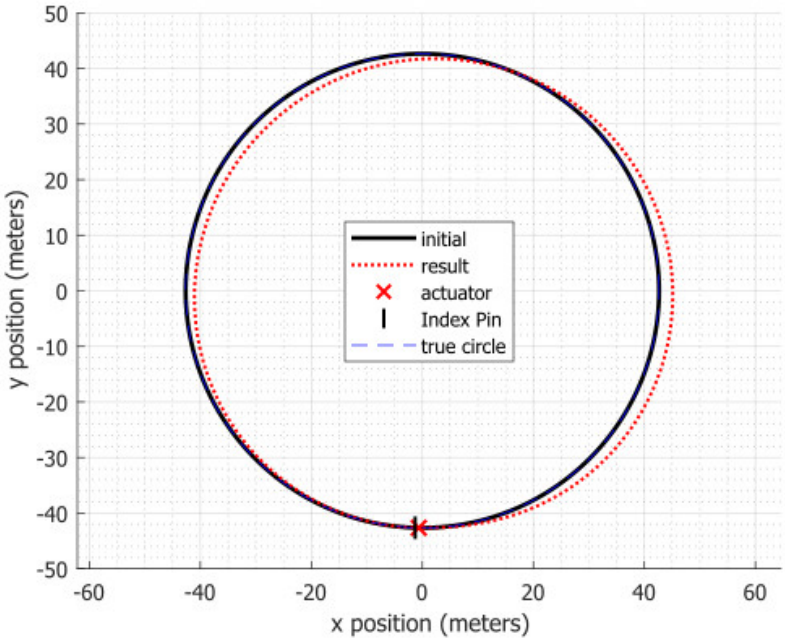

Fig. 5.2 | Deflection of the flexible structure under load, as predicted by the MATLAB FEM

5.4.2 Displacement Matrix Generation

To enable systematic analysis of structural response and actuator placement optimization, the finite element model is used to generate a comprehensive displacement matrix $\mathrm{L_{FEM}}$ that characterizes the influence of unit forces at all possible actuator locations. This matrix forms the foundation for both discrepancy modeling and actuator optimization procedures.

The displacement matrix is constructed by applying unit forces sequentially to each node in the structure and computing the resulting displacement field. For boundary conditions specified as nodes 413, 414, 164, and 171 fixed, unit force is applied at node i while maintaining zero force at all other nodes. Given the initial shape $\mathrm{x_0} \in \mathbb{R}^n$, unit force f_i applied at node i, and boundary conditions $\Delta \mathrm{x_{n-1}} = \Delta \mathrm{x_n} = 0$, the model provides the final shape $\mathrm{x_f} \in \mathbb{R}^n$.

The displacement response for each unit force application is calculated as:

$$\Delta \mathrm{x_i} = \mathrm{x_f} - \mathrm{x_0},$$
$$f_i = 1$$
$$f_j = 0, \quad \forall j \neq i$$

The displacement matrix $\mathrm{L_{FEM}}$ is then defined as:

$$\mathrm{L_{FEM}} = [\Delta \mathrm{x_1}, \Delta \mathrm{x_2} ... \Delta \mathrm{x_n}] \in \mathbb{S}^n$$

This displacement matrix provides a complete characterization of the linear structural response predicted by the finite element model. However, as discussed in the motivation, significant discrepancies typically exist between FEM predictions and experimental measurements in manufacturing environments. The following section presents a discrepancy modeling approach that systematically corrects these predictions using experimental data to achieve the accuracy required for manufacturing control applications.

5.4.3 Discrepancy Modeling Framework

To address the systematic differences between finite element predictions and experimental measurements, a discrepancy modeling framework is developed that corrects the baseline FEM using experimental data. The approach employs modal decomposition techniques combined with Bayesian estimation methods to learn corrections to the displacement matrix while maintaining computational efficiency suitable for manufacturing control applications.

The framework leverages experimental data collected from eight actuator locations distributed around the flexible structure to characterize the discrepancy between predicted and observed structural behavior. A leave-one-out cross-validation approach is employed to assess the model's ability to generalize to unseen actuator locations, ensuring robust performance across the entire structural domain.

Experimental Data Collection

High-precision experimental measurements are collected using laser tracking systems to characterize actual structural response under controlled actuation. For each of the eight actuator locations (positions 5, 6, 7, 8, 13, 14, 15, and 16), measurements consist of:

- Initial radial configuration $r_0 \in \mathbb{R}^{414}$
- Applied actuator force $a \in \mathbb{R}$
- Final radial configuration $r_{\text{final}} \in \mathbb{R}^{414}$

The true displacement response is extracted from the measurements as:

$$x_{\text{true}} = \text{LOWESS}(r_{\text{final}} - r_0, \text{frac} = 0.03) \tag{5.1}$$

where LOWESS (Locally Weighted Scatterplot Smoothing) is applied to reduce measurement noise while preserving the underlying structural response characteristics essential for model correction.

Model Correction Methodology

The discrepancy modeling approach employs a reduced-order representation of the displacement matrix combined with sequential Bayesian estimation to learn corrections from experimental data. The method initializes with the finite element displacement matrix L_{FEM} and systematically updates modal parameters based on observed discrepancies between predicted and measured responses.

Cross-validation assessment uses each actuator location as test data while the remaining seven locations provide training data for model correction. The approach retains $r = 10$ dominant modes from the finite element model and employs carefully tuned noise parameters ($\Sigma_u = 10^{-1}I$, $\Sigma_z = 10^{-3}I$) to balance model flexibility with numerical stability.

For each training measurement $(u_k, x_{\text{true},k})$, the algorithm executes a three-step process:

1. **Prediction**: Forward propagation of system state based on current model estimates

2. **Correction**: Bayesian update using observed displacement to refine model parameters

3. **Reconstruction**: Updated displacement matrix computation with enforced boundary conditions

The corrected displacement matrix is reconstructed as:

$$L_k = \Psi_r \text{diag}(\lambda_{r,k}) \Psi_r^T \tag{5.2}$$

where Ψ_r represents the retained modal basis and $\lambda_{r,k}$ are the updated eigenvalues reflecting learned corrections.

Performance Assessment

Model performance is quantified through multiple metrics that assess both prediction accuracy and uncertainty quantification capabilities. Root Mean Square Error (RMSE) provides direct comparison between corrected predictions and experimental measurements:

$$\text{RMSE} = \sqrt{\frac{1}{n} \sum_{i=1}^{n} (L_k u - x_{\text{true}})_i^2} \tag{5.3}$$

Relative improvement over baseline finite element predictions is calculated as:

$$\text{Improvement} = \frac{\text{RMSE}_{\text{FEM}} - \text{RMSE}_{\text{hybrid}}}{\text{RMSE}_{\text{FEM}}} \times 100\% \tag{5.4}$$

The framework also provides uncertainty quantification through posterior covariance estimates Σ_k, enabling confidence interval computation for both displacement predictions and model parameters. This uncertainty information is essential for manufacturing control applications where reliability requirements demand knowledge of prediction confidence bounds.

5.4.4 Discrepancy Modeling Results

Model Validation and Performance

The discrepancy modeling framework demonstrates substantial improvements in prediction accuracy compared to baseline finite element methods. Figure 5.3 illustrates the performance across all eight actuator locations during holdout validation, comparing hybrid model predictions (blue line) against experimental measurements (orange line) and pure FEM predictions (green line). The consistent outperformance of the hybrid model validates the effectiveness of the physics-data integration approach for manufacturing applications.

Quantitative performance analysis, summarized in Table 5.2, reveals an average RMSE reduction of 91.9% compared to pure FEM predictions. Seven out of eight locations demonstrate improvements exceeding 70%, with the best performance achieving 99.4% improvement at actuator angle 222.61°. The robust generalization capability is evidenced by consistent performance maintained across 306° of circumferential coverage, demonstrating the framework's reliability across the structural domain.

The single case of performance degradation at actuator angle 132.17° is attributed to sensor malfunction during data collection, highlighting the importance of robust data quality assurance in experimental validation. Despite this outlier, the overall performance demonstrates that the discrepancy modeling approach successfully bridges the gap between theoretical predictions and experimental reality.

5.5 Material Property Informed Actuator Optimization

The enhanced prediction accuracy achieved through discrepancy modeling enables more informed decisions regarding actuator placement and manufacturing system design. By incorporating experimentally-corrected material property information, the optimization of actuator configurations becomes significantly more effective than approaches based solely on nominal finite element models. This section presents methods for optimizing actuator placement using the corrected displacement matrix and demonstrates improved control performance

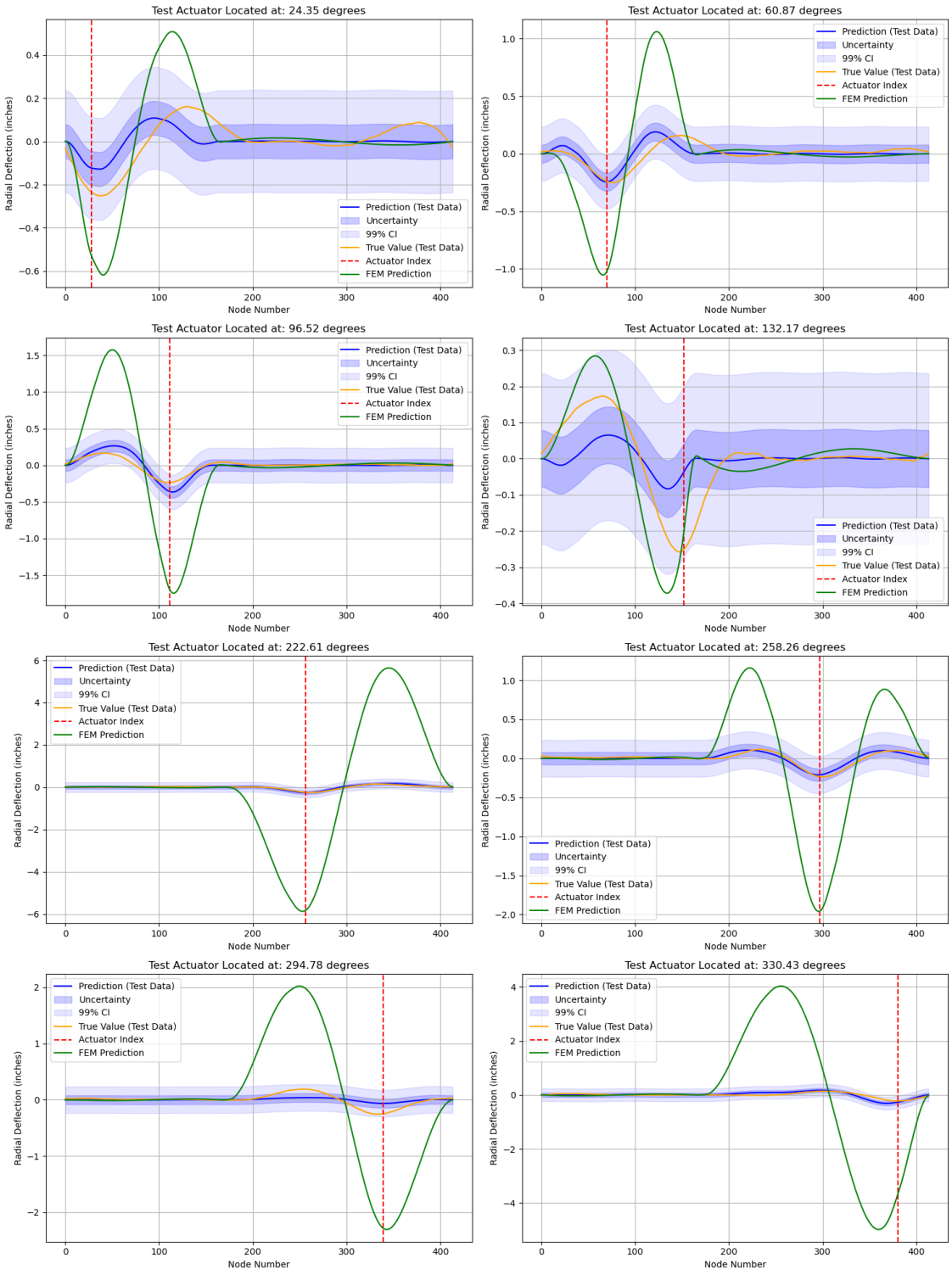

Fig. 5.3 | Discrepancy model validation Comparisons of hybrid predictions, experimental measurements, and FEM predictions across eight actuator locations show the model's ability to learn the experimental measurements.

Table 5.2: **Discrepancy Model Performance Summary**

Actuator Angle (°)	Hybrid Model RMSE	FEM RMSE	Improvement (%)
24.35	0.043	0.159	72.9
60.87	0.060	0.356	83.0
96.52	0.031	0.593	94.8
132.17	0.075	0.074	-1.7*
222.61	0.018	2.738	99.4
258.26	0.027	0.636	95.8
294.78	0.068	0.977	93.1
330.43	0.040	2.227	98.2
Average	**0.045**	**0.970**	**91.9**

*Single case of performance degradation attributed to force sensor malfunction

through data-informed design decisions.

5.5.1 QR Decomposition-Based Actuator Placement

Optimal actuator locations are identified using QR pivoting applied to the corrected displacement matrix, leveraging the improved material property understanding gained through discrepancy modeling [69, 71]. The approach begins with singular value decomposition of the displacement matrix:

$$\mathrm{L_{FEM}} = \Psi \Sigma \mathrm{V}^{\mathrm{T}}$$

This decomposition provides spatial modes Ψ and corresponding singular values Σ, as shown in Figure 5.4. The spatial modes capture the fundamental deformation patterns of the structure, while the singular values indicate the relative importance of each mode for control purposes.

For comparison with the existing experimental setup, eight actuator locations are selected

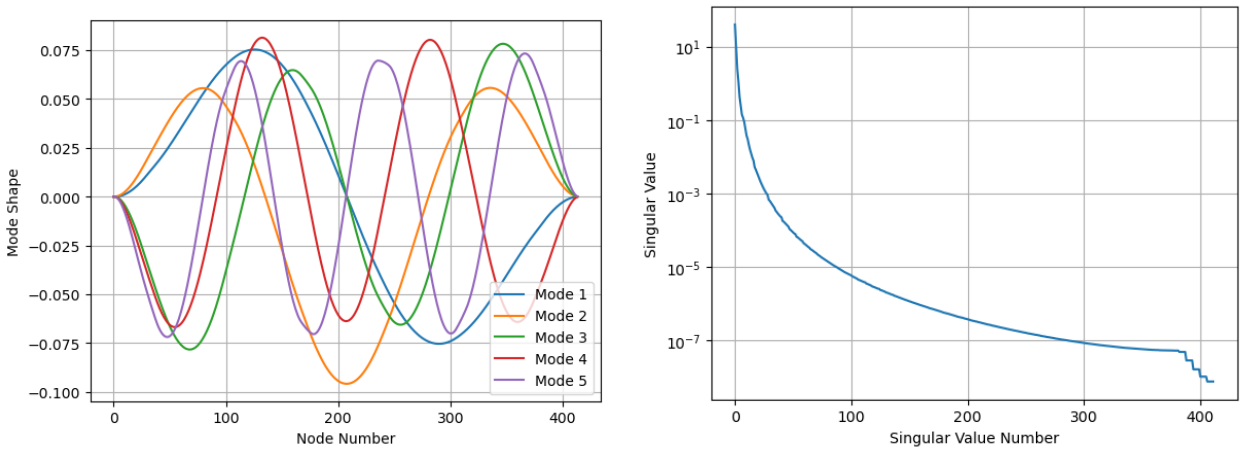

Fig. 5.4 | The first 5 modes of Ψ (left) and singular values Σ (right) of $\mathrm{L_{FEM}}$

($N_{actuators} = 8$). QR pivoting of the dominant spatial modes identifies optimal actuator placement:

$$\Psi_{\mathrm{r}}\mathrm{P}^{\mathrm{T}} = \mathrm{QR}, \quad \Psi_{\mathrm{r}} \in \mathbb{R}^{n\times 8}$$

The resulting optimized actuator locations, shown in Figure 5.5, demonstrate strategic positioning that maximizes controllability while avoiding regions of low structural response.

5.5.2 Shape Control Performance Comparison

To validate the effectiveness of material property-informed actuator optimization, shape control performance is compared between conventional actuator placement and QR-optimized configurations. The test case involves transforming an elliptical initial shape to a circular target configuration, representing a typical manufacturing correction scenario where gravitational sagging must be compensated.

The baseline approach employs convex optimization with L1 regularization to determine actuator forces:

$$\min_{\mathrm{a}} \quad \|(\mathrm{L_{FEM}} \cdot \mathrm{a} + \mathrm{x}_0) - \mathrm{x_f}\|_2 + \lambda\|\mathrm{a}\|_1$$

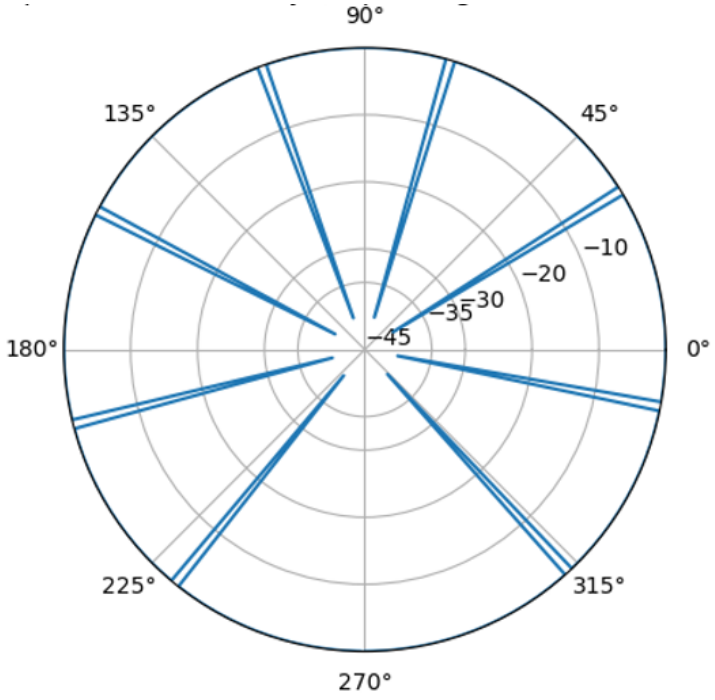

Fig. 5.5 | Optimized Locations for 8 actuators, obtained by QR Pivoting of Ψ_r

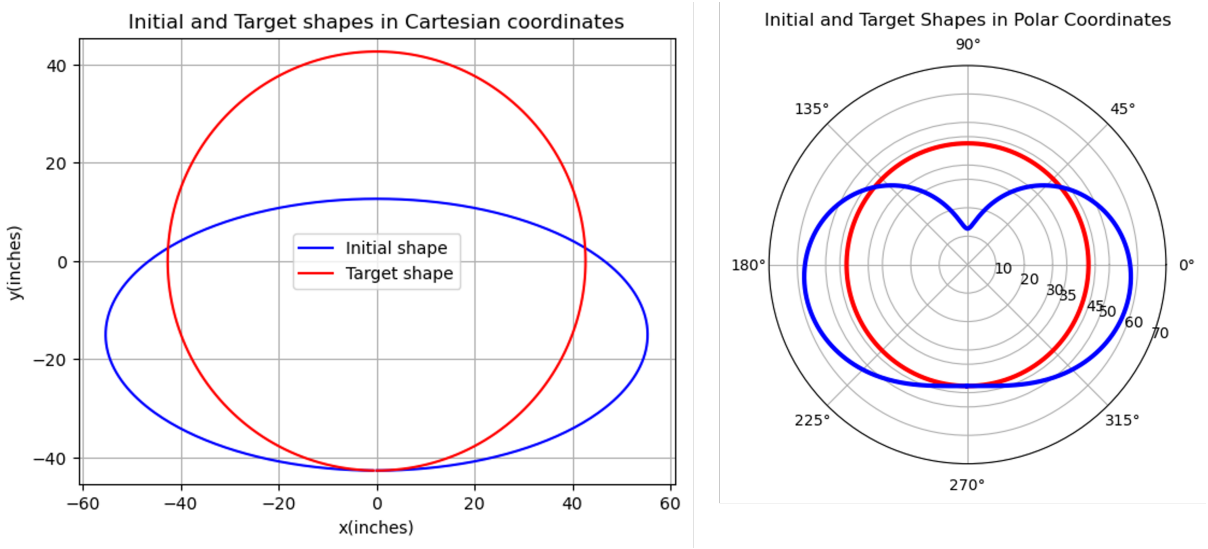

Fig. 5.6 | Initial and Target Shapes Considered for Optimal Actuator Placement

This formulation enforces perimeter conservation (a physical constraint of the flexible structure) while minimizing actuation effort. The results, shown in Figure 5.7, achieve an RMS error of 0.599 relative to the target circular shape.

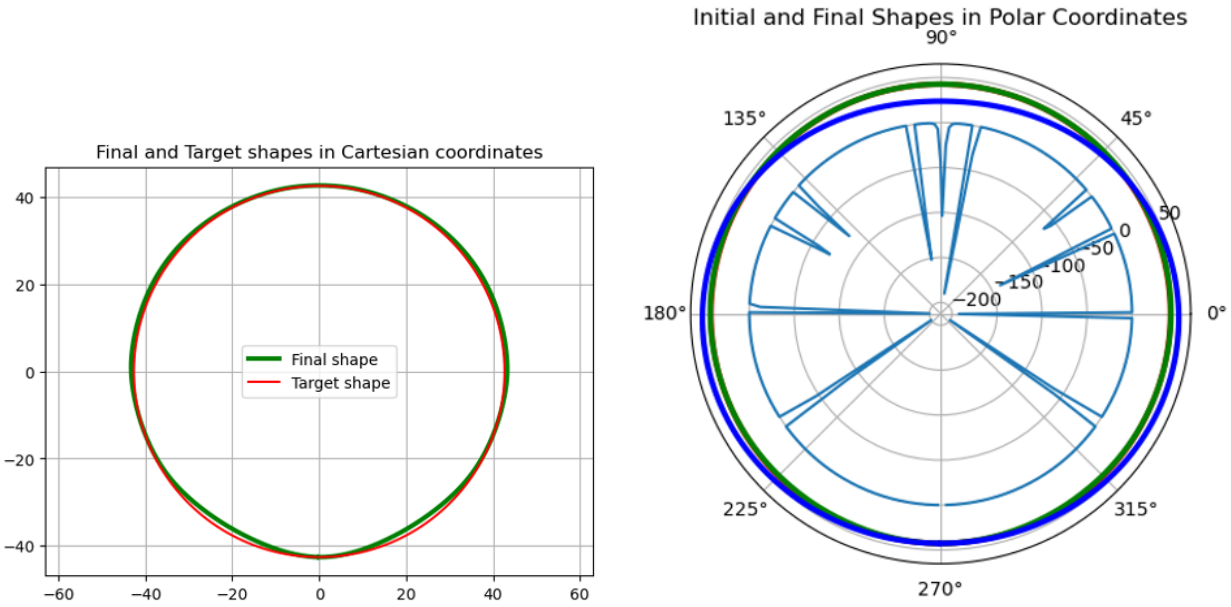

Fig. 5.7 | Shape Control Results using Conventional Approach The shape control results, with an RMS error of 0.599, are shown in Cartesian coordinates (left) and polar coordinates (right). The plot on the right also shows the locations and magnitudes of forces applied, in the interior of the polar plot.

In contrast, the QR-optimized actuator placement employs ridge regression with the reduced actuator set:

$$\min_{\mathrm{a}} \quad \|(\mathrm{L_{QR}} \cdot \mathrm{a} + \mathrm{x_{initial}}) - \mathrm{x_{final}}\|_2 + \alpha\|\mathrm{a}\|_2$$

$$\mathrm{L_{QR}} = \mathrm{L_{FEM}}\mathrm{P}^{\mathrm{T}}[:8] \in \mathbb{R}^{n\times 8}$$

The QR-optimized approach achieves significantly improved performance with an RMS

error of 0.353, representing a 41% reduction compared to conventional placement. Figure 5.8 demonstrates the superior shape control capability enabled by informed actuator positioning.

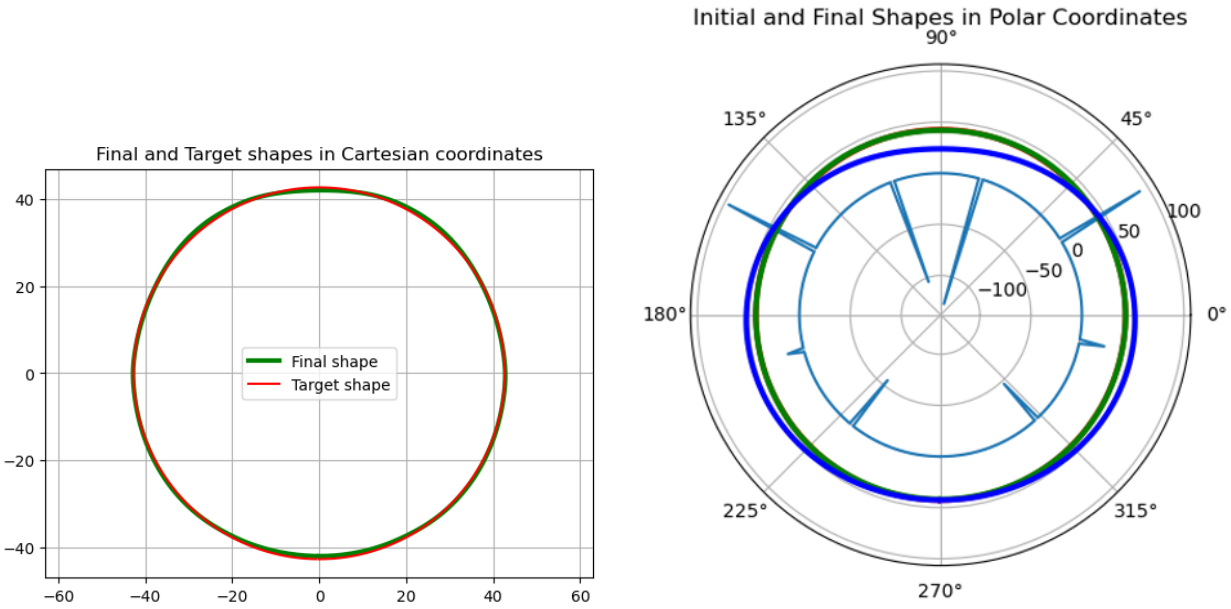

Fig. 5.8 | Shape Control Results using QR-Optimized Placement The shape control results, with an RMS error of 0.35, are shown in Cartesian coordinates (left) and polar coordinates (right). The plot on the right also shows the locations and magnitudes of forces applied, in the interior of the polar plot.

5.5.3 Integration of Material Property Knowledge and Manufacturing Design

The improved performance achieved through QR-optimized actuator placement demonstrates the value of incorporating experimentally-corrected material property information into manufacturing system design. The discrepancy modeling framework enables more accurate prediction of structural response, which in turn enables more effective optimization of actuator configurations. This creates a synergistic relationship between material charac-

terization and system design that is essential for advanced manufacturing automation.

The 41% improvement in shape control accuracy achieved through optimized actuator placement, while demonstrated for a specific ellipse-to-circle transformation, represents a general capability that extends to arbitrary shape control objectives. The QR decomposition approach identifies actuator locations that maximize controllability across the full range of achievable deformations, providing robust performance for diverse manufacturing scenarios.

Furthermore, the integration of physics-based modeling with experimental correction enables manufacturing systems to adapt to material property variations that inevitably occur in production environments. By systematically learning discrepancies between predicted and actual behavior, the framework provides a pathway for manufacturing systems to maintain high performance despite uncertainties in material properties, boundary conditions, and environmental factors.

Chapter 6

CONCLUSION AND FUTURE WORK

6.1 Data-driven Optimization of Manufacturing

This dissertation has developed a framework for data-driven optimization of manufacturing processes, addressing challenges that span from individual worker safety to large-scale structural control. The research demonstrates how sensor technologies, machine learning approaches, and hybrid physics-data modeling can be integrated to develop manufacturing systems that consider both human factors and operational performance.

6.1.1 Ergonomic Risk Assessment and Human Factors

A multimodal sensor testbed was developed for ergonomic assessment to enable objective, real-time monitoring of worker risk in hand-intensive manufacturing processes. The integration of upper body pose estimation, hand pose tracking, wrist angle measurement, and force sensing provides detailed characterization of the biomechanics of composite hand layup operations. This data collection approach enables analysis of force-motion relationships that are difficult to assess through traditional observational methods.

Machine learning models for automated prediction of industry-standard RULA and HAL scores achieved over 95% classification accuracy while generalizing to unseen participants. This capability addresses limitations of traditional ergonomic assessment methods, including inter-rater variability, labor-intensive evaluation procedures, and limited real-time feedback capabilities. These predictive models demonstrate the feasibility of continuous, objective ergonomic monitoring in industrial environments.

The Biometric Assessment of Complete Hand (BACH) score was introduced as a new ergonomic assessment metric. By incorporating wrist torque calculations relative to biome-

chanical capacity and accounting for angle-dependent strength variations, BACH provides more detailed assessment of hand and finger risks compared to existing metrics. The sensitivity of BACH to specific hand motions and force applications enables targeted ergonomic interventions and workplace optimization strategies.

The application of ergonomic insights to shop aide redesign demonstrates the translation of research findings into workplace improvements. By using BACH scoring as an optimization objective, the research establishes a framework for evidence-based tool design that can reduce ergonomic risk while maintaining manufacturing effectiveness. This approach enables proactive risk prevention through data-informed design decisions.

6.1.2 Human Factors and Manufacturing Automation

The research establishes connections between ergonomic assessment and manufacturing automation, examining how human factors considerations drive automation needs while informing automation system design. The multimodal dataset collected for ergonomic assessment provides insights into the biomechanics of skilled manufacturing operations, creating resources for robotic end effector development and control strategy optimization.

The analysis indicates that composite hand layup presents ergonomic risks that cannot be fully addressed through workplace modifications alone, suggesting automation as a potential safety intervention. The temporal analysis of RULA, HAL, and BACH scores throughout layup operations shows that risk exposure occurs throughout the entire process, making comprehensive ergonomic intervention challenging without fundamental changes to the manufacturing approach.

The transition from human-scale manipulation to large-scale structural control illustrates the application of data-driven approaches across different manufacturing domains. While hand-intensive processes may benefit from automation to reduce ergonomic risks, large-scale manufacturing faces different challenges related to material property uncertainties and structural behavior prediction. This recognition motivated the development of modeling approaches that can address the gap between computational predictions and physical reality.

6.1.3 Physics-Informed Modeling and Hybrid Approaches

A discrepancy modeling framework was developed that combines finite element analysis with experimental measurements to address limitations of traditional computational approaches in manufacturing environments. The systematic correction of physics-based models using experimental data achieved an average 91.9% reduction in prediction error compared to baseline finite element methods, indicating improvements possible through hybrid modeling approaches.

The framework maintains computational efficiency while achieving improved prediction accuracy, making it suitable for real-time manufacturing control applications. The use of modal decomposition and Bayesian estimation techniques enables the approach to learn systematic corrections from limited experimental data while providing uncertainty quantification for manufacturing applications where reliability requirements necessitate confidence bounds on predictions.

The generalization capability demonstrated across multiple actuator locations indicates the framework's applicability to diverse manufacturing scenarios. The consistent performance maintained across 306° of circumferential coverage provides evidence of the approach's reliability for potential industrial implementation.

6.1.4 Material Property-Informed System Optimization

The integration of experimentally-corrected material property information with actuator optimization shows improvements in manufacturing system performance. The QR decomposition-based approach to actuator placement, informed by the corrected displacement matrix, achieved a 41% improvement in shape control accuracy compared to conventional placement strategies. This result indicates the value of incorporating accurate material understanding into manufacturing system design decisions.

The optimization approach identifies actuator configurations that improve system controllability while considering hardware requirements and installation complexity. The method-

ology for determining both the number and spatial distribution of actuators provides a framework that can be adapted to diverse structural control applications in manufacturing environments.

The relationship between accurate modeling and effective control demonstrates the potential of integrated approaches to manufacturing system design. By combining physics-based understanding with experimental validation, the framework enables manufacturing systems to achieve improved control performance while adapting to material property variations and manufacturing uncertainties that occur in production environments.

6.1.5 Manufacturing Optimization Framework

The research establishes a framework for data-driven manufacturing optimization that addresses challenges across multiple scales and domains. The progression from individual worker safety through automation design to large-scale structural control illustrates the interconnected nature of modern manufacturing challenges and the potential benefits of integrated solution approaches.

The methodological contributions include sensor integration, machine learning model development, hybrid physics-data modeling, and optimization techniques. These methods are unified by their emphasis on using experimental data to improve system performance while maintaining practical constraints including computational efficiency, implementation complexity, and industrial reliability requirements.

The framework's consideration of both human factors and system performance represents an approach to manufacturing optimization that recognizes the relationship between worker safety, product quality, and operational efficiency. This perspective is relevant for developing manufacturing systems that can meet demands for customization, quality, and productivity while maintaining safe work environments.

The validation of the framework across diverse applications—from ergonomic assessment to structural control—indicates its broad applicability and establishes a foundation for future work in intelligent manufacturing systems. The research provides practical benefits through

deployable technologies and methodological contributions that can guide future research in data-driven manufacturing optimization.

Together, these contributions establish a foundation for data-driven manufacturing optimization that considers both human factors and system performance, representing an approach to addressing contemporary challenges in composite manufacturing while providing a methodological framework for future work in intelligent manufacturing systems.

6.2 Further Verification of the Discrepancy Model and Optimized Actuation

6.2.1 Robotic Validation Platform

To further validate and extend the discrepancy modeling framework developed in Chapter 5, a robotic experimental platform is proposed that enables systematic evaluation of the hybrid modeling approach under controlled conditions. The robotic setup provides precise, repeatable actuation that eliminates variability associated with manual force application, enabling more rigorous validation of the discrepancy model predictions.

Figure 6.1 illustrates the proposed robotic validation platform, featuring a flexible structure similar to the composite barrel used in the original experiments, but equipped with precision robotic actuators capable of applying controlled forces at specified locations. The robotic platform enables systematic exploration of the force-displacement relationship across the entire structural domain, providing comprehensive datasets for model validation and refinement.

6.2.2 Extended Discrepancy Model Applications

The robotic platform enables extension of the discrepancy modeling approach to more complex loading scenarios and boundary conditions. Multi-actuator coordination experiments can evaluate the model's performance under simultaneous actuation at multiple locations, representing more realistic control scenarios. Dynamic loading experiments assess the model's applicability to time-varying force applications, extending beyond the quasi-static

Fig. 6.1 | Robotic validation platform for discrepancy model verification showing flexible structure with robotic actuators

assumptions of the current framework.

The controlled nature of robotic actuation facilitates systematic uncertainty quantification studies, enabling characterization of model performance across different force magnitudes, actuation patterns, and boundary conditions. These studies provide critical insights into the model's operational domain and reliability bounds, informing deployment decisions for real-world applications.

6.2.3 Optimized Actuator Placement Validation

The robotic platform provides an ideal testbed for validating the optimal actuator placement strategies developed using QR decomposition methods. Movable robotic actuators can be positioned at the theoretically optimal locations identified through the controllability analysis, enabling direct comparison with alternative placement strategies.

The robotic platform enables precise measurement of shape control accuracy, force requirements, and control authority for each configuration, providing quantitative validation of the optimization approach. The integration of the discrepancy model with optimal actuator placement represents a comprehensive framework for adaptive shape control of flexible structures. The robotic validation platform serves as a bridge between theoretical development and practical implementation, providing the experimental foundation necessary for technology transfer to industrial applications.

BIBLIOGRAPHY

[1] ACGIH. Threshold limit values for chemical substances and physical agents and biological exposure indices. In *American Conference of Governmental Industrial Hygienists*. ACGIH Worldwide, 2001.

[2] Panagiotis Aivaliotis, Konstantinos Georgoulias, Zoi Arkouli, and Sotiris Makris. Methodology for enabling digital twin using advanced physics-based modelling in predictive maintenance. *Procedia Cirp*, 81:417–422, 2019.

[3] Panagiotis Aivaliotis, Konstantinos Georgoulias, and George Chryssolouris. The use of digital twin for predictive maintenance in manufacturing. *International Journal of Computer Integrated Manufacturing*, 32(11):1067–1080, 2019.

[4] Thomas J Armstrong, Lawrence J Fine, Steven A Goldstein, Yair R Lifshitz, and Barbara A Silverstein. Ergonomics considerations in hand and wrist tendinitis. *The Journal of Hand Surgery*, 12(5):830–837, 1987.

[5] EM Bezerra, MS Bento, JAFF Rocco, K Iha, VL Lourenço, and LC Pardini. Artificial neural network (ann) prediction of kinetic parameters of (crfc) composites. *Computational Materials Science*, 44(2):656–663, 2008.

[6] Tom Brown, Benjamin Mann, Nick Ryder, Melanie Subbiah, Jared D Kaplan, Prafulla Dhariwal, Arvind Neelakantan, Pranav Shyam, Girish Sastry, Amanda Askell, et al. Language models are few-shot learners. *Advances in neural information processing systems*, 33:1877–1901, 2020.

[7] J Brüning, Berend Denkena, M-A Dittrich, and T Hocke. Machine learning approach for optimization of automated fiber placement processes. *Procedia CIRP*, 66:74–78, 2017.

[8] Steven L Brunton and J Nathan Kutz. *Data-driven science and engineering: Machine learning, dynamical systems, and control*. Cambridge University Press, 2022.

[9] Steven L Brunton, J Nathan Kutz, Krithika Manohar, Aleksandr Y Aravkin, Kristi Morgansen, Jennifer Klemisch, Nicholas Goebel, James Buttrick, Jeffrey Poskin, Adriana W Blom-Schieber, et al. Data-driven aerospace engineering: reframing the industry with machine learning. *AIAA Journal*, 59(8):2820–2847, 2021.

[10] Steven L Brunton, Joshua L Proctor, and J Nathan Kutz. Discovering governing equations from data by sparse identification of nonlinear dynamical systems. *Proceedings of the National Academy of Sciences*, 113(15):3932–3937, 2016.

[11] Murray Campbell, A Joseph Hoane Jr, and Feng-hsiung Hsu. Deep blue. *Artificial intelligence*, 134(1-2):57–83, 2002.

[12] Emmanuel J Candès, Xiaodong Li, Yi Ma, and John Wright. Robust principal component analysis? *Journal of the ACM (JACM)*, 58(3):1–37, 2011.

[13] Harish Chander, Reuben F Burch, Purva Talegaonkar, David Saucier, Tony Luczak, John E Ball, Alana Turner, Sachini NK Kodithuwakku Arachchige, Will Carroll, Brian K Smith, et al. Wearable stretch sensors for human movement monitoring and fall detection in ergonomics. *International Journal of Environmental Research and Public Health*, 17(10):3554, 2020.

[14] Prasad Vilas Chanekar, Nikhil Chopra, and Shapour Azarm. Optimal actuator placement for linear systems with limited number of actuators. In *2017 American Control Conference (ACC)*, pages 334–339, Seattle, WA, USA, May 2017. IEEE.

[15] Alphonse Chapanis. The international ergonomics association: its first 30 years. *Ergonomics*, 33(3):275–282, 1990.

[16] Alphonse Chapanis. *Human factors in systems engineering*. John Wiley & Sons, Inc., 1996.

[17] Chun-Teh Chen and Grace X Gu. Machine learning for composite materials. *MRs Communications*, 9(2):556–566, 2019.

[18] Chun-Teh Chen and Grace X Gu. Generative deep neural networks for inverse materials design using backpropagation and active learning. *Advanced Science*, 7(5):1902607, 2020.

[19] Gengxiang Chen, Yingguang Li, Xu Liu, Charyar Mehdi-Souzani, Qinglu Meng, Jing Zhou, and Xiaozhong Hao. Physics-guided neural operator for data-driven composites manufacturing process modelling. *Journal of Manufacturing Systems*, 70:217–229, 2023.

[20] Kyunghyun Cho, Bart Van Merriënboer, Caglar Gulcehre, Dzmitry Bahdanau, Fethi Bougares, Holger Schwenk, and Yoshua Bengio. Learning phrase representations using rnn encoder-decoder for statistical machine translation. *arXiv preprint arXiv:1406.1078*, 2014.

[21] Junyoung Chung, Caglar Gulcehre, KyungHyun Cho, and Yoshua Bengio. Empirical evaluation of gated recurrent neural networks on sequence modeling. *arXiv preprint arXiv:1412.3555*, 2014.

[22] Emily Clark, J. Nathan Kutz, and Steven L. Brunton. Sensor Selection With Cost Constraints for Dynamically Relevant Bases. *IEEE Sensors Journal*, 20(19):11674–11687, October 2020.

[23] Jose Antonio Diego-Mas and Jorge Alcaide-Marzal. Using Kinect™ sensor in observational methods for assessing postures at work. *Applied Ergonomics*, 45(4):976–985, 2014.

[24] Salvatore Digiesi, Andrea Lucchese, and Carlotta Mummolo. A 'speed—difficulty—accuracy' model following a general trajectory motor task with spatial constraints: An information-based model. *Applied Sciences*, 10(21):7516, 2020.

[25] Alican Dogan and Derya Birant. Machine learning and data mining in manufacturing. *Expert Systems with Applications*, 166:114060, 2021.

[26] Juan Du, Xiaowei Yue, Jeffrey H Hunt, and Jianjun Shi. Optimal placement of actuators via sparse learning for composite fuselage shape control. *Journal of Manufacturing Science and Engineering*, 141(10):101004, 2019.

[27] M. Sajjad Edalatzadeh, Dante Kalise, Kirsten A. Morris, and Kevin Sturm. Optimal actuator design for vibration control based on LQR performance and shape calculus, March 2019. arXiv:1903.07572 [math].

[28] Michael Elkington, D Bloom, C Ward, A Chatzimichali, and K Potter. Hand layup: Understanding the manual process. *Advanced Manufacturing: Polymer & Composites Science*, 1(3):138–151, 2015.

[29] Hao-Shu Fang, Jiefeng Li, Hongyang Tang, Chao Xu, Haoyi Zhu, Yuliang Xiu, Yong-Lu Li, and Cewu Lu. AlphaPose: Whole-body regional multi-person pose estimation and tracking in real-time. *IEEE Transactions on Pattern Analysis and Machine Intelligence*, 2022.

[30] Alfred Franzblau, Thomas J Armstrong, Robert A Werner, and Sheryl S Ulin. A cross-sectional assessment of the ACGIH TLV for hand activity level. *Journal of Occupational Rehabilitation*, 15:57–67, 2005.

[31] HUILONG FU, CALEB SCHOENHOLZ, PAULINA PORTALES, AMIRALI ESKANDARIYUN, and NAVID ZOBEIRY. Accelerating composite cure cycle optimization with combined probabilistic machine learning and finite element process simulation. In *PROCEEDINGS OF THE AMERICAN SOCIETY FOR COMPOSITES-THIRTY-EIGHTH TECHNICAL CONFERENCE*, 2023.

[32] Frank Bunker Gilbreth and Lillian Moller Gilbreth. *Applied motion study: A collection of papers on the efficient method to industrial preparedness*. Macmillan, 1919.

[33] Moritz Glatt, Chantal Sinnwell, Li Yi, Sean Donohoe, Bahram Ravani, and Jan C Aurich. Modeling and implementation of a digital twin of material flows based on physics simulation. *Journal of Manufacturing Systems*, 58:231–245, 2021.

[34] Mikell P Groover. *Fundamentals of modern manufacturing: materials, processes, and systems*. John Wiley & Sons, 2010.

[35] Grace X Gu, Chun-Teh Chen, and Markus J Buehler. De novo composite design based on machine learning algorithm. *Extreme Mechanics Letters*, 18:19–28, 2018.

[36] Grace X Gu, Chun-Teh Chen, Deon J Richmond, and Markus J Buehler. Bioinspired hierarchical composite design using machine learning: simulation, additive manufacturing, and experiment. *Materials Horizons*, 5(5):939–945, 2018.

[37] Hussein Haggag, Mohammed Hossny, Saeid Nahavandi, and Douglas Creighton. Real time ergonomic assessment for assembly operations using Kinect. In *2013 UKSim 15th International Conference on Computer Modelling and Simulation*, pages 495–500. IEEE, 2013.

[38] SG Hancock and KD Potter. The use of kinematic drape modelling to inform the hand lay-up of complex composite components using woven reinforcements. *Composites Part A: Applied Science and Manufacturing*, 37(3):413–422, 2006.

[39] Carisa Harris, Ellen A Eisen, Robert Goldberg, Niklas Krause, and David Rempel. 1st place, premus best paper competition: workplace and individual factors in wrist tendinosis among blue-collar workers–the San Francisco study. *Scandinavian Journal of Work, Environment & Health*, 37(2):85, 2011.

[40] Kaiming He, Xiangyu Zhang, Shaoqing Ren, and Jian Sun. Deep residual learning for image recognition. In *Proceedings of the IEEE conference on computer vision and pattern recognition*, pages 770–778, 2016.

[41] André Heining, Kevin Schmidt, Ulrich Schönhoff, and Oliver Sawodny. Optimal Actuator Placement for the High-Precision Control of Quasi-Static Elastic Plates. *IEEE Transactions on Control Systems Technology*, 31(6):2608–2619, November 2023.

[42] Sue Hignett and Lynn McAtamney. Rapid entire body assessment (reba). *Applied Ergonomics*, 31(2):201–205, 2000.

[43] Sepp Hochreiter and Jürgen Schmidhuber. Long short-term memory. *Neural Computation*, 9(8):1735–1780, 1997.

[44] Katherine RS Holzbaur, Wendy M Murray, and Scott L Delp. A model of the upper extremity for simulating musculoskeletal surgery and analyzing neuromuscular control. *Annals of Biomedical Engineering*, 33:829–840, 2005.

[45] Zhenyu Jiang, Zhong Zhang, and Klaus Friedrich. Prediction on wear properties of polymer composites with artificial neural networks. *Composites Science and Technology*, 67(2):168–176, 2007.

[46] Osmo Karhu, Pekka Kansi, and Iikka Kuorinka. Correcting working postures in industry: A practical method for analysis. *Applied ergonomics*, 8(4):199–201, 1977.

[47] Maksims Kazijevs and Manar D. Samad. Deep imputation of missing values in time series health data: A review with benchmarking. *Journal of Biomedical Informatics*, 144:104440, 2023.

[48] Sang-Young Kim, Chun Sik Shim, Caleb Sturtevant, Dave (Dae-Wook) Kim, and Ha Cheol Song. Mechanical properties and production quality of hand-layup and vacuum infusion processed hybrid composite materials for GFRP marine structures. *International Journal of Naval Architecture and Ocean Engineering*, 6(3):723–736, 2014.

[49] Diederik P Kingma and Jimmy Ba. Adam: A method for stochastic optimization. *arXiv preprint arXiv:1412.6980*, 2014.

[50] Theresa Kleine, Julia L. Wagner, Michael Böhm, and Oliver Sawodny. Optimal actuator placement and static load compensation for a class of distributed parameter systems. *at - Automatisierungstechnik*, 69(9):739–749, September 2021.

[51] Alex Krizhevsky, Ilya Sutskever, and Geoffrey E Hinton. Imagenet classification with deep convolutional neural networks. *Advances in neural information processing systems*, 25, 2012.

[52] Raghu Raja Pandiyan Kuppusamy, Satyajit Rout, and Kaushik Kumar. Chapter one - advanced manufacturing techniques for composite structures used in aerospace industries. In Kaushik Kumar and J. Paulo Davim, editors, *Modern Manufacturing Processes*, Woodhead Publishing Reviews: Mechanical Engineering Series, pages 3–12. Woodhead Publishing, 2020.

[53] David S Landes. The unbound prometheus. *Cambridge Books*, 2003.

[54] Wendi A Latko, Thomas J Armstrong, James A Foulke, Gary D Herrin, Randall A Rabourn, and Sheryl S Ulin. Development and evaluation of an observational method for assessing repetition in hand tasks. *American Industrial Hygiene Association Journal*, 58(4):278–285, 1997.

[55] Yann LeCun, Yoshua Bengio, and Geoffrey Hinton. Deep learning. *nature*, 521(7553):436–444, 2015.

[56] Jay Lee, Behrad Bagheri, and Hung-An Kao. A cyber-physical systems architecture for industry 4.0-based manufacturing systems. *Manufacturing Letters*, 3:18–23, 2015.

[57] Kyung-Sun Lee and Myung-Chul Jung. Ergonomic evaluation of biomechanical hand function. *Safety and Health at Work*, 6(1):9–17, 2015.

[58] Sujee Lee, Li Liu, Robert Radwin, and Jingshan Li. Machine learning in manufacturing ergonomics: Recent advances, challenges, and opportunities. *IEEE Robotics and Automation Letters*, 6(3):5745–5752, 2021.

[59] KB Lim. Method for optimal actuator and sensor placement for large flexible structures. *Journal of Guidance, Control, and Dynamics*, 15(1):49–57, 1992.

[60] Hod Lipson and Melba Kurman. *Fabricated: The new world of 3D printing*. John Wiley & Sons, 2013.

[61] Yanglong Lu, Eduard Shevtshenko, and Yan Wang. Physics-based compressive sensing to enable digital twins of additive manufacturing processes. *Journal of Computing and Information Science in Engineering*, 21(3):031009, 2021.

[62] Andrea Lucchese, Salvatore Digiesi, Kübra Akbaş, and Carlotta Mummolo. An agent-specific stochastic model of generalized reaching task difficulty. *Applied Sciences*, 11(10):4330, 2021.

[63] Andrea Lucchese, Salvatore Digiesi, and Carlotta Mummolo. Analytical-stochastic model of motor difficulty for three-dimensional manipulation tasks. *Plos one*, 17(10):e0276308, 2022.

[64] J Luo, Z Liang, C Zhang, and B Wang. Optimum tooling design for resin transfer molding with virtual manufacturing and artificial intelligence. *Composites Part A: applied science and manufacturing*, 32(6):877–888, 2001.

[65] Shuaiyin Ma, Wei Ding, Yang Liu, Shan Ren, and Haidong Yang. Digital twin and big data-driven sustainable smart manufacturing based on information management systems for energy-intensive industries. *Applied energy*, 326:119986, 2022.

[66] Pankar K Mallick. *Fiber-reinforced composites: materials, manufacturing, and design*. CRC press, 2007.

[67] Vito Modesto Manghisi, Antonio Emmanuele Uva, Michele Fiorentino, Vitoantonio Bevilacqua, Gianpaolo Francesco Trotta, and Giuseppe Monno. Real time RULA assessment using Kinect v2 sensor. *Applied Ergonomics*, 65:481–491, 2017.

[68] Henry B Mann and Donald R Whitney. On a test of whether one of two random variables is stochastically larger than the other. *The annals of mathematical statistics*, pages 50–60, 1947.

[69] Krithika Manohar, Bingni W Brunton, J Nathan Kutz, and Steven L Brunton. Data-driven sparse sensor placement for reconstruction: Demonstrating the benefits of exploiting known patterns. *IEEE Control Systems Magazine*, 38(3):63–86, 2018.

[70] Krithika Manohar, Thomas Hogan, Jim Buttrick, Ashis G Banerjee, J Nathan Kutz, and Steven L Brunton. Predicting shim gaps in aircraft assembly with machine learning and sparse sensing. *Journal of Manufacturing Systems*, 48:87–95, 2018.

[71] Krithika Manohar, J Nathan Kutz, and Steven L Brunton. Optimal sensor and actuator selection using balanced model reduction. *IEEE Transactions on Automatic Control*, 67(4):2108–2115, 2021.

[72] Chris C Martin, Dan C Burkert, Kyung R Choi, Nick B Wieczorek, Patrick M McGregor, Richard A Herrmann, and Peter A Beling. A real-time ergonomic monitoring system using the Microsoft Kinect. In *2012 IEEE Systems and Information Engineering Design Symposium*, pages 50–55. IEEE, 2012.

[73] Elton Mayo. *The human problems of an industrial civilization*. Routledge, 2004.

[74] MRH Mazumder, P Govindaraj, and N Salim. Digitalization of composite manufacturing using nanomaterials-based piezoresistive sensors. *Elsevier*, 2024.

[75] Lynn McAtamney and Nigel Corlett. Rapid upper limb assessment (RULA). In *Handbook of Human Factors and Ergonomics Methods*, pages 86–96. CRC Press, 2004.

[76] Matt Middlesworth. The most important benefit of maintaining a neutral posture. `https://www.ergo-plus.com/the-most-important-benefit-of-maintaining-a-neutral-posture/`, 2023. [Online; accessed 7-Nov-2023].

[77] Douglas C Montgomery. *Introduction to statistical quality control*. John wiley & sons, 2020.

[78] Srimantha E Mudiyanselage, Phuong Hoang Dat Nguyen, Mohammad Sadra Rajabi, and Reza Akhavian. Automated workers' ergonomic risk assessment in manual material handling using sEMG wearable sensors and machine learning. *Electronics*, 10(20):2558, 2021.

[79] Ahmed Mujtaba, Faisal Islam, Patrick Kaeding, Thomas Lindemann, and B Gangadhara Prusty. Machine-learning based process monitoring for automated composites manufacturing. *Journal of Intelligent Manufacturing*, 36(2):1095–1110, 2025.

[80] Nipun D Nath, Reza Akhavian, and Amir H Behzadan. Ergonomic analysis of construction worker's body postures using wearable mobile sensors. *Applied Ergonomics*, 62:107–117, 2017.

[81] Nipun D Nath, Theodora Chaspari, and Amir H Behzadan. Automated ergonomic risk monitoring using body-mounted sensors and machine learning. *Advanced Engineering Informatics*, 38:514–526, 2018.

[82] Tamara Nestorović and Miroslav Trajkov. Optimal actuator and sensor placement based on balanced reduced models. *Mechanical Systems and Signal Processing*, 36(2):271–289, 2013.

[83] Occupational Safety and Health Administration. *OSHA Technical Manual (OTM)*. U.S. Department of Labor, Washington, D.C. Available at `https://www.osha.gov/otm`, Accessed: 2025-07-16.

[84] Igiri Onaji, Divya Tiwari, Payam Soulatiantork, Boyang Song, and Ashutosh Tiwari. Digital twin in manufacturing: conceptual framework and case studies. *International journal of computer integrated manufacturing*, 35(8):831–858, 2022.

[85] Peter O'donovan, Kevin Leahy, Ken Bruton, and Dominic TJ O'Sullivan. Big data in manufacturing: a systematic mapping study. *Journal of Big Data*, 2:1–22, 2015.

[86] Sharon L Padula and Rex K Kincaid. Optimization strategies for sensor and actuator placement. Technical report, 1999.

[87] Behnoosh Parsa and Ashis G Banerjee. A multi-task learning approach for human activity segmentation and ergonomics risk assessment. In *Proceedings of the IEEE/CVF Winter Conference on Applications of Computer Vision*, pages 2352–2362, 2021.

[88] Behnoosh Parsa, Ekta U Samani, Rose Hendrix, Cameron Devine, Shashi M Singh, Santosh Devasia, and Ashis G Banerjee. Toward ergonomic risk prediction via segmentation of indoor object manipulation actions using spatiotemporal convolutional networks. *IEEE Robotics and Automation Letters*, 4(4):3153–3160, 2019.

[89] Hanchuan Peng, Fuhui Long, and Chris Ding. Feature selection based on mutual information criteria of max-dependency, max-relevance, and min-redundancy. *IEEE Transactions on Pattern Analysis and Machine Intelligence*, 27(8):1226–1238, 2005.

[90] Pierre Plantard, Hubert PH Shum, Anne-Sophie Le Pierres, and Franck Multon. Validation of an ergonomic assessment method using Kinect data in real workplace conditions. *Applied Ergonomics*, 65:562–569, 2017.

[91] Robert G Radwin, David P Azari, Mary J Lindstrom, Sheryl S Ulin, Thomas J Armstrong, and David Rempel. A frequency–duty cycle equation for the ACGIH hand activity level. *Ergonomics*, 58(2):173–183, 2015.

[92] TG Ritto and FA Rochinha. Digital twin, physics-based model, and machine learning applied to damage detection in structures. *Mechanical Systems and Signal Processing*, 155:107614, 2021.

[93] Mohammad Reza Sadeghi, Seyed Mohammad Hosseini Varkiyani, and Ali Asghar Asgharian Jeddi. Machine learning in optimization of nonwoven fabric bending rigidity in spunlace production line. *Scientific Reports*, 13(1):17702, 2023.

[94] Gavriel Salvendy. *Handbook of human factors and ergonomics*. John Wiley & Sons, 2012.

[95] Mark C Schall Jr, Nathan B Fethke, and Victoria Roemig. Digital human modeling in the occupational safety and health process: An application in manufacturing. *IISE transactions on occupational ergonomics and human factors*, 6(2):64–75, 2018.

[96] Peter J Schmid. Dynamic mode decomposition of numerical and experimental data. *Journal of Fluid Mechanics*, 656:5–28, 2010.

[97] Michael Schmidt and Hod Lipson. Distilling free-form natural laws from experimental data. *Science*, 324(5923):81–85, 2009.

[98] Gennaro Senatore, Francesco Virgili, and Lucio Blandini. Global optimal actuator placement for adaptive structures: New formulation and benchmarking. *Journal of Intelligent Material Systems and Structures*, 36(3):151–173, February 2025.

[99] Michael Sharp, Ronay Ak, and Thomas Hedberg Jr. A survey of the advancing use and development of machine learning in smart manufacturing. *Journal of manufacturing systems*, 48:170–179, 2018.

[100] David Silver, Aja Huang, Chris J Maddison, Arthur Guez, Laurent Sifre, George Van Den Driessche, Julian Schrittwieser, Ioannis Antonoglou, Veda Panneershelvam, Marc Lanctot, et al. Mastering the game of go with deep neural networks and tree search. *nature*, 529(7587):484–489, 2016.

[101] Elena Stefana, Filippo Marciano, Diana Rossi, Paola Cocca, and Giuseppe Tomasoni. Wearable devices for ergonomics: A systematic literature review. *Sensors*, 21(3):777, 2021.

[102] Nenad Stojanovic and Dejan Milenovic. Data-driven digital twin approach for process optimization: An industry use case. In *2018 IEEE International Conference on Big Data (Big Data)*, pages 4202–4211. IEEE, 2018.

[103] Tyler H. Summers, Fabrizio L. Cortesi, and John Lygeros. On Submodularity and Controllability in Complex Dynamical Networks. *IEEE Transactions on Control of Network Systems*, 3(1):91–101, March 2016.

[104] Tyler H Summers and John Lygeros. Optimal sensor and actuator placement in complex dynamical networks. *IFAC Proceedings Volumes*, 47(3):3784–3789, 2014.

[105] Shahriar Talebi, Amirhossein Taghvaei, and Mehran Mesbahi. Data-driven optimal filtering for linear systems with unknown noise covariances. *Advances in Neural Information Processing Systems*, 36:69546–69585, 2023.

[106] Fei Tao, Qinglin Qi, Ang Liu, and Andrew Kusiak. Data-driven smart manufacturing. *Journal of Manufacturing Systems*, 48:157–169, 2018.

[107] Frederick Winslow Taylor. *Scientific management*. Routledge, 2004.

[108] V. Tzoumas, M. A. Rahimian, G. J. Pappas, and A. Jadbabaie. Minimal Actuator Placement With Bounds on Control Effort. *IEEE Transactions on Control of Network Systems*, 3(1):67–78, March 2016.

[109] U.S. Bureau of Labor Statistics. Injuries, Illnesses, and Fatalities (IIF) Program. `https://www.bls.gov/iif/`. Accessed: 2025-07-16.

[110] Manish T Valoor and K Chandrashekhara. A thick composite-beam model for delamination prediction by the use of neural networks. *Composites science and technology*, 60(9):1773–1779, 2000.

[111] A Vaswani. Attention is all you need. *Advances in Neural Information Processing Systems*, 2017.

[112] Mario Vega-Barbas, Jose A Diaz-Olivares, Ke Lu, Mikael Forsman, Fernando Seoane, and Farhad Abtahi. P-Ergonomics Platform: Toward precise, pervasive, and personalized ergonomics using wearable sensors and edge computing. *Sensors*, 19(5):1225, 2019.

[113] Julia L. Wagner, Kevin Schmidt, Michael Böhm, and Oliver Sawodny. Optimal Actuator Placement and Static Load Compensation for Euler-Bernoulli Beams with Spatially Distributed Inputs. *IFAC-PapersOnLine*, 52(15):489–494, 2019.

[114] Xingzhi Wang, Yuchen Wang, Fei Tao, and Ang Liu. New paradigm of data-driven smart customisation through digital twin. *Journal of manufacturing systems*, 58:270–280, 2021.

[115] Yi Wang, Siyuan Chen, Iryna Tretiak, Stephen R Hallett, and Jonathan P-H Belnoue. Virtual data-driven optimisation for zero defect composites manufacture. *Materials & Design*, 241:112934, 2024.

[116] Bernd Waschneck, André Reichstaller, Lenz Belzner, Thomas Altenmüller, Thomas Bauernhansl, Alexander Knapp, and Andreas Kyek. Optimization of global production scheduling with deep reinforcement learning. *Procedia Cirp*, 72:1264–1269, 2018.

[117] Thomas R Waters, Vern Putz-Anderson, Arun Garg, and Lawrence J Fine. Revised niosh equation for the design and evaluation of manual lifting tasks. *Ergonomics*, 36(7):749–776, 1993.

[118] Thorsten Wuest, Daniel Weimer, Christopher Irgens, and Klaus-Dieter Thoben. Machine learning in manufacturing: advantages, challenges, and applications. *Production & Manufacturing Research*, 4(1):23–45, 2016.

[119] Charles Yang, Youngsoo Kim, Seunghwa Ryu, and Grace X Gu. Prediction of composite microstructure stress-strain curves using convolutional neural networks. *Materials & Design*, 189:108509, 2020.

[120] Zhenze Yang, Chi-Hua Yu, and Markus J Buehler. Deep learning model to predict complex stress and strain fields in hierarchical composites. *Science Advances*, 7(15):eabd7416, 2021.

[121] Heecheon You and Ochae Kwon. A survey of repetitiveness assessment methodologies for hand-intensive tasks. *International journal of industrial ergonomics*, 35(4):353–360, 2005.

[122] Xiaowei Yue, Yuchen Wen, Jeffrey H Hunt, and Jianjun Shi. Active learning for gaussian process considering uncertainties with application to shape control of composite fuselage. *IEEE Transactions on Automation Science and Engineering*, 18(1):36–46, 2020.

[123] Clemens Zimmerling, Dominik Dörr, Frank Henning, and Luise Kärger. A machine learning assisted approach for textile formability assessment and design improvement of composite components. *Composites Part A: Applied Science and Manufacturing*, 124:105459, 2019.

[124] Clemens Zimmerling, Christian Poppe, and Luise Kärger. Estimating optimum process parameters in textile draping of variable part geometries-a reinforcement learning approach. *Procedia manufacturing*, 47:847–854, 2020.

[125] Clemens Zimmerling, Daniel Trippe, Benedikt Fengler, and Luise Kärger. An approach for rapid prediction of textile draping results for variable composite component geometries using deep neural networks. In *AIP conference proceedings*. AIP Publishing, 2019.